



UNIVERSITAT DE  
BARCELONA

**MASTER THESIS**

# **First Night Sky Modelling of Montsec protected area**

Master in Astrophysics, Cosmology and Particle Physics  
2016-2017

Author: Hector Linares

Advisors: Dr. Eduard Masana (UB-ICC-IEEC)

Dr. Salvador J. Ribas (PAM)

Collab.: Dr. Manuel García (Dpt. Sostenibilitat i Territori,  
Generalitat de Catalunya)



## **ABSTRACT**

The purposes of this thesis are to build a tool that can be used easily in the future to evaluate: the effect and propagation, in astronomical units, of a given set of light; and the impact in light pollution that changes in the lighting system produce. Afterwards once this tool is developed and tested we will use it: to study the modifications in light pollution produced in Lleida due to a change in the lighting system, and to discover the level of light pollution that Lleida is producing as seen from the *Parc Astronòmic del Montsec* (PAM).

The tool used is divided in two parts. The first one relies on the Illumina model developed by the group of Dr. M. Aubé [1]. This model requires a detailed input of the surrounding area such as topographic information, a detailed inventory of the lights with its features inside the region of study and information about atmospheric conditions. The second part is developed in Matlab and its function is to convert the output of Illumina to magnitudes to obtain similar astronomic results to measurements on the field such as all-sky ASTMON images [7].

The results show that the model built is working properly. Lleida is affecting observations made from the PAM in some lines of sight as suspected by the astronomers. The results agree with the measurements taking into account the simplification made. The lighting system change in Lleida show a shift in wavelength of light emitted with an increase in some wavelength related to the blue light.

## **ACKNOWLEDGEMENTS**

I want to thank the thorough work of my advisors Dr. Masana and Dr. Salvador Ribas (PAM) for the support and long hours looking for the roots of some troubles we were having. I want also to thank and Dr. Manuel García, of the Sostenibility Department of the Generalitat de Catalunya, as well as Dr. Martin Aubé and Alexandre Simoneau, from the Illumina project, for their insights, interest and availability along the whole project.

Finally there are two groups that worth an acknowledgment that are the city council of Lleida and the company Citelum for the information provided. Without it, it could not have been possible to get accurate results.



# CONTENTS

Introduction.....	1
1.Light pollution .....	2
1.1.Light pollution effects .....	2
1.2.Light propagation.....	2
1.3.Lighting system properties.....	4
1.3.1.Light Spectrum .....	4
1.3.2.Light output pattern .....	5
2. Methodology.....	6
2.1.Illumina .....	6
2.1.1.Input files.....	6
2.1.2.Case of study variables.....	8
2.1.3.Computation.....	8
2.1.4.Contribution to Illumina project.....	9
2.2.Post-processing.....	10
2.2.1.Filters B-V-R .....	10
2.2.2.Apparent magnitudes .....	11
3. Case of study: Montsec Observatory .....	11
3.1.PAM (Parc Astronòmic del Montsec).....	12
3.2.Lleida .....	12
3.3.Computation variables.....	16
4.Results .....	17
4.1.Apparent magnitudes and colors .....	17
4.2.Comparison between inventories .....	20
4.3.Discussion .....	24
5.Conclusions.....	25
6. References.....	26
Appendix .....	27

## Introduction

Studies on the effects of light pollution show that this phenomenon have a direct impact to the environment, wildlife and could as well affect human health by changing the natural light cycle. Light pollution is also detrimental because is a contributor to climate change through unnecessary energy consumption. Fortunately, the global increasing awareness and the conviction to ameliorate artificial light emission make the study on light pollution very popular. Nowadays it is taking a new perspective with the combination of different kind of measurements with modelling of light propagation.

This project aims to develop a tool to better understand what kind of sources produces light pollution and how they affect astronomic studies. It measures light pollution in the Johnson's visual filters B-V-R, frequently used in astronomy, in any line of sight from the observer. Besides astronomical implication, it will be useful for cities and towns to help in choosing properly the lighting system to be installed or replaced to reduce their light pollution.

The tool developed will be used in this paper to evaluate the light pollution that is receiving the Parc Astronòmic del Montsec (PAM) from Lleida, the biggest city around located approximately 50km south from the PAM. Montsec area is an astronomical protected area labelled as Reference Point in Catalonia and certified as Starlight Reserve. This case of study will be interesting not only for the relevance of the PAM but to compare the effects of two different lighting systems. In 2014 Lleida updated its light inventory mostly by replacing mercury vapor and some metal halide lights by LEDs.

The first building block of the tool is based on the Illumina program developed by Dr. Martin Aubé et al. It computes the spectral flux produced in the line of sight of the observer taking as an input the topography, night light emittance and ground reflectance of the region studied, atmospheric parameters and information about the lighting systems of the cities and villages around the observer. While working with Illumina we contributed to the well-functioning of the code. The second building block is developed in Matlab and its function is to convert the output of Illumina to astronomical magnitudes to build all-sky maps similar to the ones obtained by ASTMOM.

The results show that Lleida is affecting the measurements of the night-sky made from the PAM. The polluted line of sights are concentrated at low elevation angles and around the azimuth of Lleida. The change in the lighting system in Lleida shifted the light to different wavelengths being particularly interesting for its implications a huge increase around the peak of sensitivity of the scotopic light at 515nm.

The division and order of this paper ensures its well understanding. First section explains the reasons that motivates this project, the second one how the tool works, the third one describes the PAM-Lleida case of study and finally the results obtained are displayed.

# 1. Light pollution

## 1.1. Light pollution effects

During last century cities, towns and civilization as a whole have experienced a brightening of the night. Beyond its obvious benefits such as safety, better driving conditions and extended productive hours, it carried major drawbacks not only for astronomy, decreasing the number of observable phenomena as showed in Figure 1, but also for the environment, energy consumption and even affecting our health.

Astronomers have been pushed out from big cities in order to have a better sight of the night sky. Nowadays almost every observatory is located in an isolated environment in an effort to reduce light pollution from its studies, however it is frequently impossible to avoid it completely, as happens in the Montsec observatory, case of study of this thesis. Ecosystems and wildlife are also affected by light pollution. Almost all life on Earth has adapted to the light cycle of day and night, enlightening the night affect life-sustaining behaviors such as reproduction, nourishment, sleep and protection from predators. Humans are not an exception, and research suggests that artificial light at night can negatively affect human health because it affects the circadian rhythm, a sleep-wake pattern governed by the day-night cycle, our bodies produce the hormone melatonin in response to that rhythm, which helps keep us healthy because it has antioxidant properties, induces sleep, boosts the immune system, lowers cholesterol, and helps the functioning of several organs. Its alteration, being particularly accentuated by exposure to the blue light could lead to increasing risks for obesity, depression, sleep disorders, diabetes, breast cancer and more. Another drawback of light pollution is the increase in energy consumption, directly related with lighting power. The international dark-sky association (IDA) estimates that 30 percent of all outdoor lighting in the U.S. is wasted, that adds up to \$3.3 billion and the release of 21 million tons of carbon dioxide per year. To offset all that carbon dioxide, we'd have to plant 875 million trees annually. [2]

With much of the Earth's population living under light-polluted skies (see Figure 2), over lighting is an international concern. According to the 2016 groundbreaking "World Atlas of Artificial Night Sky Brightness" [10], 80 percent of the world's population lives under skyglow. In the United States and Europe 99 percent of the public can't experience a natural night. [2]

Light pollution affects every citizen. Fortunately, concern about light pollution is rising dramatically. A growing number of scientists, homeowners, environmental groups and civic leaders are taking action to restore the natural night.

## 1.2. Light propagation

Any kind of light source can produce light pollution, if it is received in the line of sight of the observer without being the target of the observation. Light do not always follow a straight path in the atmosphere, it can change its direction several times (figure 3). We can divide the received light by its path:



Figure 1. Before and during the 2003 Northeast blackout, a massive power outage that affected 55 million people. Photo by of Todd Carlson [2]



Figure 2. Satellite night view of the Earth [3]

- Direct light: the light source is aligned with the line of sight.
- First order scattered light: the light from the source is projected towards the sky and a part of this light is returned back towards the observer by the atmospheric constituents (molecules and aerosols).
- Second air scattered light: as first air scattered light but changing the direction of the light beam more than once.
- Ground reflected light: light projected to the ground is reflected by it and oriented to the line of sight or towards the sky and then deviated by atmospheric constituents to the observer. Ground reflected light is considered as first and second order scattering depending on the number of scattering in the air.

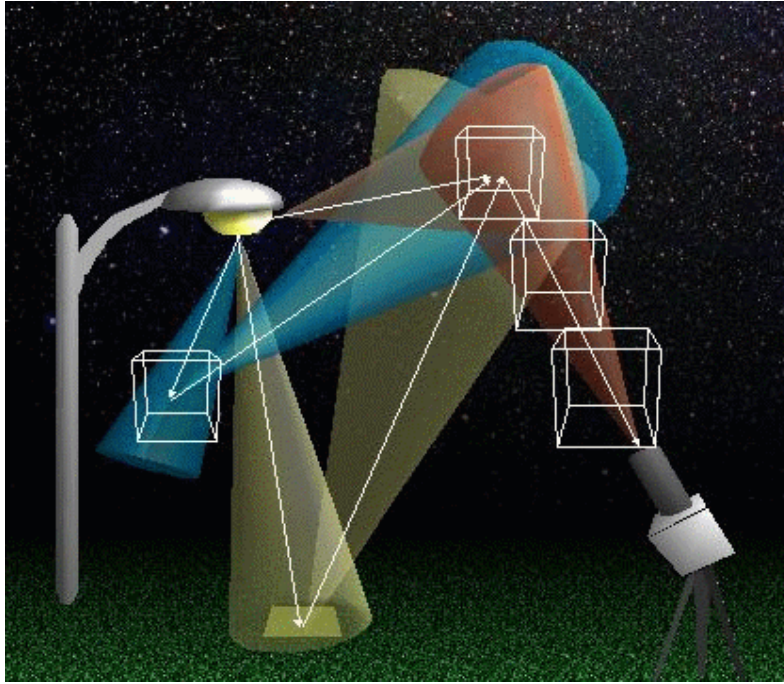


Figure 3. Some paths of light propagation [1]

It is obvious then that atmospheric conditions and ground properties affect the impact of light pollution.

### 1.3. Lighting system properties

#### 1.3.1. Light Spectrum

The spectrum of a lamp is defined as the distribution of its emitted light along the electromagnetic spectrum<sup>1</sup>. Visible light is just a little fraction of this electromagnetic spectrum but even tiny changes in the wavelength are perceived by the human eye. These changes in wavelength is what define the colors that we see, and they are related with the temperature of the lamp. As can be seen in figure 4 hotter the lamp bluer the light. Blue light is particularly harmful for human health as explained and unfortunately most LEDs emit in this wavelength. In the present, in order to reduce the energy consumption mercury vapor or sodium vapor lamps are being replaced for LEDs, but it could not carry a healthier light environment.

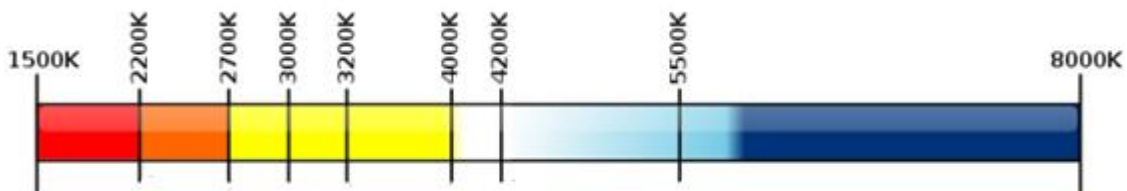


Figure 4. Kelvin temperature chart. Credit:  
[http://commons.wikimedia.org/wiki/File:Kelvin\\_Temperature\\_Chart.svg](http://commons.wikimedia.org/wiki/File:Kelvin_Temperature_Chart.svg)

<sup>1</sup> See Appendix A.1. to see some light spectrums.

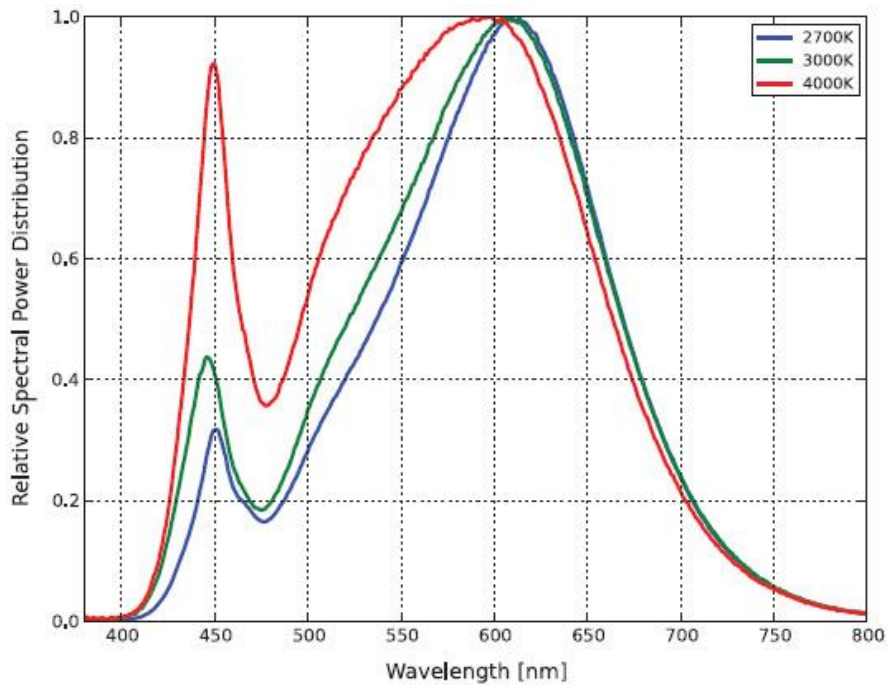


Figure 5. Spectrum of the light emitted from a LED operating at different temperatures. At low wavelength (blue light) the emission increases with temperature

### 1.3.2. Light output pattern

Light output pattern (LOP) of lamps is one of the most important variables in light pollution. It is the angular distribution of the emitting light. LOP should vary to fulfill the illumination needs of each scenario but it may not go beyond the target area.

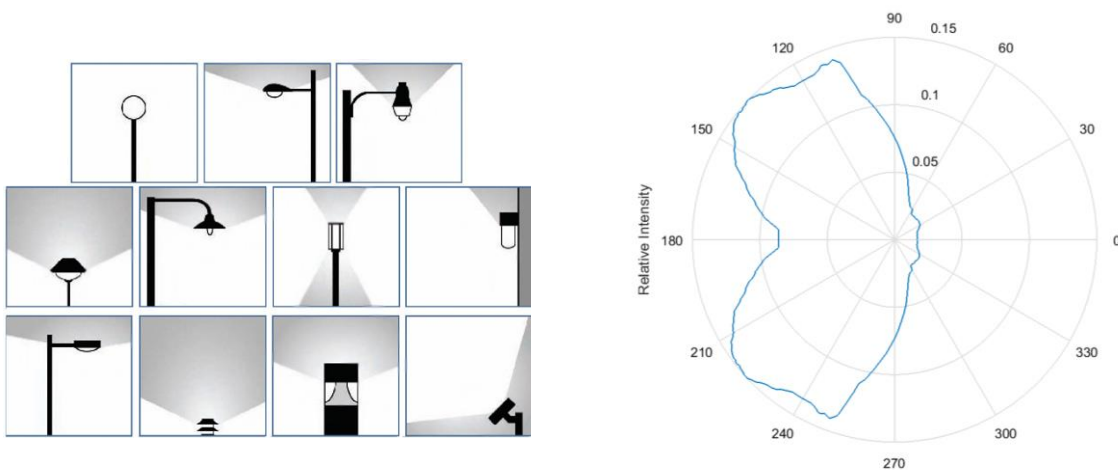


Figure 6. Left: lighting systems with different LOP. Right: LOP of a lamp with 20% of light emitted upwards represented in an angular distribution plot ( $0^\circ$  zenith pointing to the right).

## 2. Methodology

The methodology used in this project to compute the light pollution received by the observer from the surroundings is divided in two main blocks. The first one is the Illumina program [1] [6], an open source code developed by Martin Aubé et al. that produces several outputs regarding atmospheric conditions and light pollution, for our purposes the output needed is the luminance received in selected directions from the point of view of the observer. The second block is the post-processing, developed in Matlab, which consists in the conversion to proper astronomic magnitudes and its display in order to obtain a similar output that the one obtained by measures on the field, hence being able to compare both of them if needed.

### 2.1. Illumina

Illumina is a sophisticated light pollution numerical model able to simulate with precision human induced sky radiance under a variety of conditions. The novelty of this model lies in the fact that it makes it possible to take account of the heterogeneity of the environment in addition to being able to simulate the spectral behavior of the phenomenon. In order to explain the Illumina code images from a provided example located in the Hawaii islands are displayed [11].

#### 2.1.1. Input files

##### *Domain definition*

Illumina requires to define the location where the study will take place indicating two opposite corners of the region. It is necessary also to define the coordinate system used to define the corners and the size in meters of each pixel.

##### *Satellite data*

There are three different kind of satellite data of the region defined needed to run Illumina: the night light emittance obtained from VIIRS imagery; a digital elevation model made with the SRTM elevation data; and the ground reflectance at multiple wavelength obtained from Modis imagery.

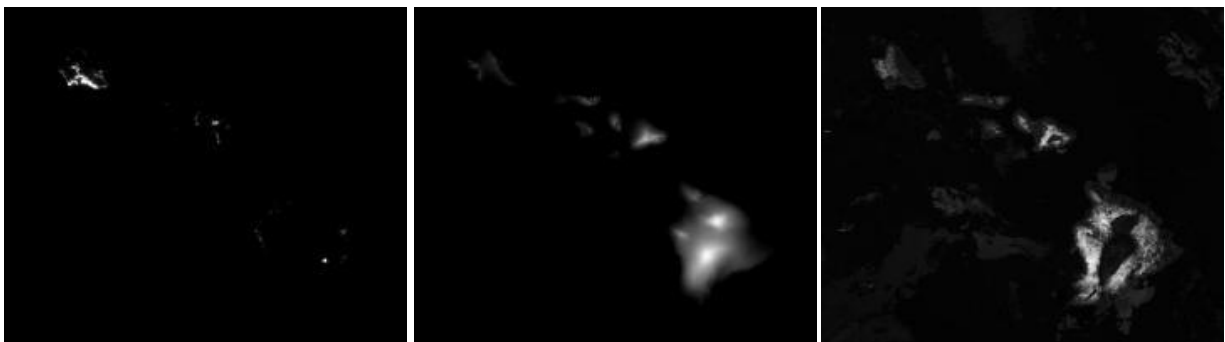


Figure 7. Left: Night emittance. Centre: digital elevation of the Hawaii Islands. Right: ground reflectance. All images are from Hawaii Islands

### Light inventory

For each emitting light zone to be considered it is needed to define its location within the domain, its radius, the mean vertical and horizontal distance between obstacles, the mean height of its lamps, and the percentage of its lamps (spectrum) and its LOP, allowing to combine several of them.

In the example there are defined 5 zones. One of them is inside another zone, and another one is empty of lights in order to show the possibilities and function of the program. Figure 9 is the inventory where all the data can be observed: the first and second columns are the location of the center of each zone in pixels (px), the third column its radius in px, fourth and fifth are the distance to obstacles in meters, sixth the obstacle filling factor, seventh the mean height of the lamps and eighth the inventory of lights. The inventory of lights has the format X\_A\_Y, being A the spectrum of the light, Y the LOP and X the percentage respect to the total of the combination of A and Y. As an example the first zone has 90% of Halogenous with a LOP emitting 5% of the flux upwards and 10% of Metal Halide with a LOP emitting 10% upwards [11].



Figure 8. Zones of the example showed with freemaptools

#	x'	y'	R	hobs	dobs	fobs	hlamp	Zone inventory	Comment
90	325	50	7	25	0.5	7	90_H_5 10_M_10	# Oahu	
190	277	40	7	25	0.5	7	90_H_5 10_M_10	# Molokai + Lanai	
280	253	64	7	25	0.5	7	18_H_10 72_H_0 10_M_10	# Maui	
343	129	103	7	25	0.5	7	87_L_10 8_H_10 5_M_5	# Big Island	
381	90	23	7	25	0.5	7	0_L_0	# Lava	

Figure 9. Light inventory of the zones.

With the previous data Illumina creates a unique light emission profile for each zone averaging by its weight the spectrum and LOP of every lights inside the zone, see figure 10. From here on the code will use this equivalent profile as a light source with the dimensions of the zone where it belongs.

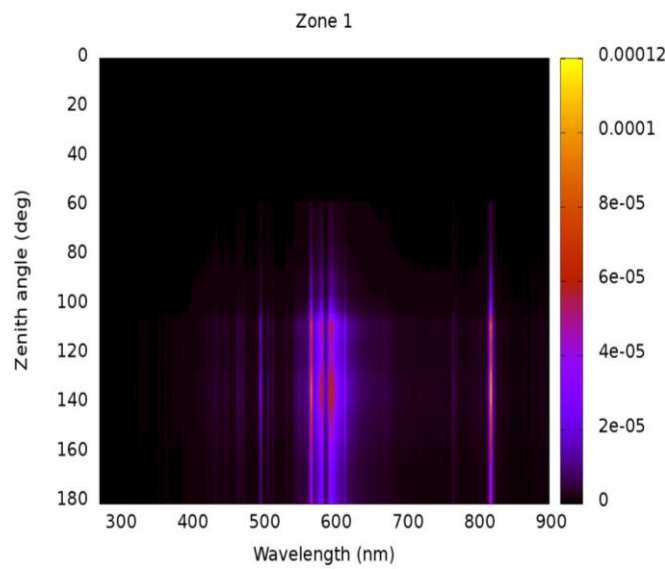


Figure 10. Light emission model for the zone 1 of Hawaii example. Most of the light is emitted downwards in the wavelength around 580nm

### 2.1.2. Case of study variables

Once the scenario is defined the code requires specific parameters for experiment to be performed.

- Wavelength range: maximum and minimum wavelength to study and the number of windows to divide it.
- Atmospheric parameters: aerosol characterization, there are several environments such as rural, maritime, etc.; the level of relative humidity; kind of clouds present; aerosol optical depth; angstrom coefficients.
- Position of the observer: the location in px of the observer as well as its height.
- Lines of sight: elevation and azimuth angles.
- Computation parameters: resolution radii, scattering radius, contribution limiting factor and second scattering acceleration factor.

### 2.1.3. Computation

For each line of sight the total spectral flux  $F$  (Watt/nm) received by the observer is given by [4]:

$$\Phi = \sum_n I_{no} \Omega_{no} \frac{\Omega_{on}}{\Omega_{FOV}} \quad (1)$$

Here  $I_{no}$  is the light spectral intensity (W/str/nm) scattered toward the observer by a model cell crossed by the observer line of sight;  $\Omega_{no}$  is the solid angle subtended by the observer as seen from scattering cell  $n$  (see Figure 11);  $\Omega_{on}$  is the solid angle subtended by cell  $n$  as seen from the observer position  $o$ ;  $\Omega_{FOV}$  is the solid angle of the observer field of view (FOV). The model takes the sum over  $n$  to integrate the light scattered along the line of sight.

The model assume that  $I_{no}$  is mainly explained by the combination of the first-order scattering  $I_1$  and  $I_{r1}$  (with and without reflection on the ground) and the second-order scattering  $I_2$  and  $I_{r2}$ .

Light extinction arising during various light paths between the light source and the observer is computed. To enable this computation, it is assumed that the vertical profiles of the molecular and aerosol concentrations follow exponentially decreasing functions. It is also assumed that aerosol and molecular concentration profiles are uniform over the modeling domain.

Ground reflectance is assumed to be Lambertian. The computation of the reflected light goes up to a maximum reflective radius (MRR) centered on each lighting ground cell. MRR represents the free light path towards the ground, which is determined by the presence of obstacles, such as trees, buildings or topography.

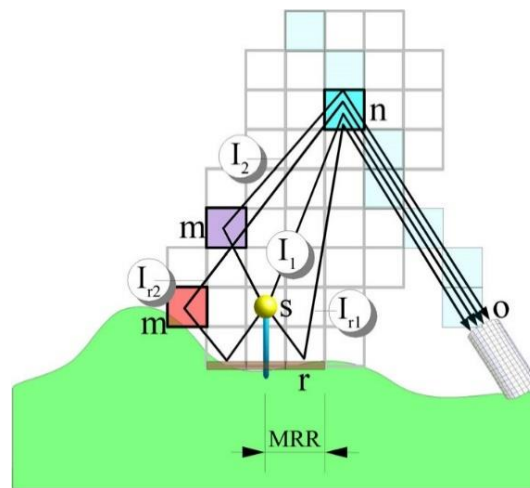


Figure 11. Scheme of the model used by Illumina to compute the spectral Flux received in each direction

#### 2.1.4. Contribution to Illumina project

Illumina is a quite new model and thus there are very few studies relying on it, our project is one of the first performed out of the developing group. While working with Illumina we pointed out some misunderstandings in the user's guide that were gathered and corrected in an update by Martin Aubé et al. see [12].

We also discovered some bugs in the code never found before, some of them just because our compiler were less permissive than the used by the developers but two of them were clearly important. The first one consisted in the program stops computing when the line of sight pointed to a light zone and the distance to the observer was very close to the distance to that zone. The second one was related with how the distance increases to compute the first and second order scattering light, the step was big enough to avoid some significant contribution to the light pollution, this problem produced the contra intuitive result that we were receiving less spectral flux in the direction of the light zone.

## 2.2. Post-processing

Illumina was designed to simulate the light scattered back to a spectrometer, so the output is spectral flux, hard to compare it with astronomical on site measurements. Besides, the model only simulates the contribution of artificial light to the night-sky glow. Contributions from moonlight, auroras, stars, the Milky Way and any other celestial objects are not taken into account.

The post-processing program aimed to go further and convert the output in astronomical magnitudes in the visible B-V-R Johnson's Filters taking into account the natural brightness of night sky.

### 2.2.1. Filters B-V-R

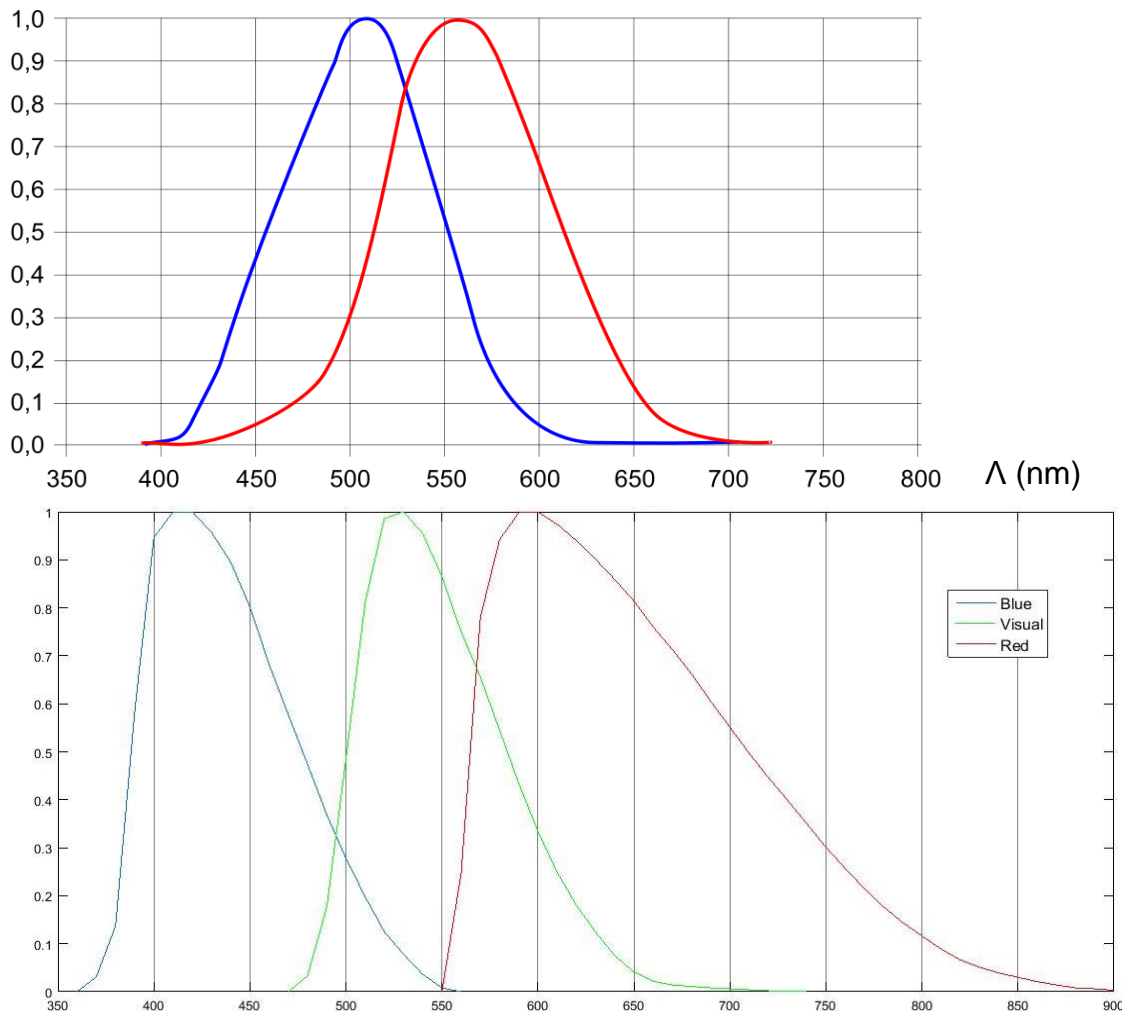


Figure 12. Top: human scotopic (blue) and photopic sensitivity (red)<sup>2</sup>. Bottom: B-V-R Johnson filters.

<sup>2</sup> De HHahn - CC BY-SA 3.0, <https://commons.wikimedia.org/w/index.php?curid=9058334>

Johnson's filters is a photometric system that consists in several passbands that covers a significant range in the electromagnetic spectrum. For the purposes of the study only those that covers the visual range will be used B, V and R, which stands for Blue, Visual and Red respectively. The sensitivity of the human vision can be divided in photopic, in good lighting conditions as day-light, and scotopic, in bad lighting condition as at night. See the relation between them in figure 12.

In order to compute the flux in each of the filters we need to make the convolution between the filter function and the spectral flux received. To do so we have to discretize both functions by the same step, multiply them and integrate the result for the filter domain. We have used the Simpson's method to integrate the resulting function, see section 3.3 for details with the sampling in wavelength.

### 2.2.2. Apparent magnitudes

Apparent magnitudes are defined by the following expression:

$$m = m_{ref} - 2.5 * \log_{10} \left( \frac{F}{F_{ref}} \right) \quad (2)$$

The reference object used is Vega star because of its well-known spectrum and apparent magnitude in each filter [15].

To obtain the apparent magnitude in the Johnson's filters we compute the flux for the computed light pollution and for Vega for each of the filters using the method explained in 2.2.1.

Once known the Vega's flux in each of the filters we can compute the contribution of the natural night sky using the magnitudes tabulated in table 1 using equation 2 in the form:

$$F = F_{ref} * 10^{(0.4 * (m_{ref} - m))} \quad (3)$$

After converting the light pollution spectral flux computed by Illumin to flux, we finally add the light pollution flux and the flux from the night sky in order to compare the results with measurements taken on the field:

$$m_{obs} = m_V - 2.5 * \log_{10} \left( \frac{F_{LP} + F_{NNS}}{F_V} \right) \quad (4)$$

Table 1. Apparent magnitudes of Vega and natural sky brightness [14]

Johnson Filter	Vega	Natural Sky
B	-0.023	22.7
V	-0.023	21.8
R	-0.023	20.9

### 3. Case of study: Montsec Observatory

#### 3.1. PAM (Parc Astronòmic del Montsec)

PAM is a scientific center focused in astronomy. Its main purposes are research, formation and dissemination of this field. Its main facilities are the Universe Observatory Center (COU) and the Astronomic Observatory of Montsec (OAdM).

It is located 50km north from Lleida, the biggest city around it, see figure 13. Some scientific studies certified this location as ideal for astronomic purposes due to its low level of pluviometry and humidity, the high ratio of clear nights and its elevation, around 1600m above sea level.

Regarding light pollution, the sky above the PAM was considered as free from light pollution because only lights close to the horizon are detected and hence it is protected by the local legal framework [5].



Figure 13. Location of the PAM

However, there are some towns around the Park that are actually affecting astronomical measurements. In particular Lleida is thought to be one of the major stakeholders polluting the sky above PAM.

#### 3.2. Lleida

Lleida is located around  $190^\circ$  in azimuth ( $0^\circ$  pointing to the North) at 47 km from the PAM. It is a middle-sized city with almost 140.000 inhabitants, with an extension of approximately 220 km<sup>2</sup>.

Lleida is affecting the measurements taken from the PAM in some lines of sights and it's visible to the naked eye from there.

Beyond the significance of studying how the city is affecting the sky over the observatory, it is relevant due to an update of the lighting system of the city that took place in 2014. This allows us to study the resulting modifications in light pollution and validate the model in both scenarios.

We had access to the real inventory of lights before and after the 2014 courtesy by the city council of Lleida and Citelum. The information provided for each light source included: emitted power, kind of light source, height, percentage of light emitted upwards and location in coordinates (see figure 14).

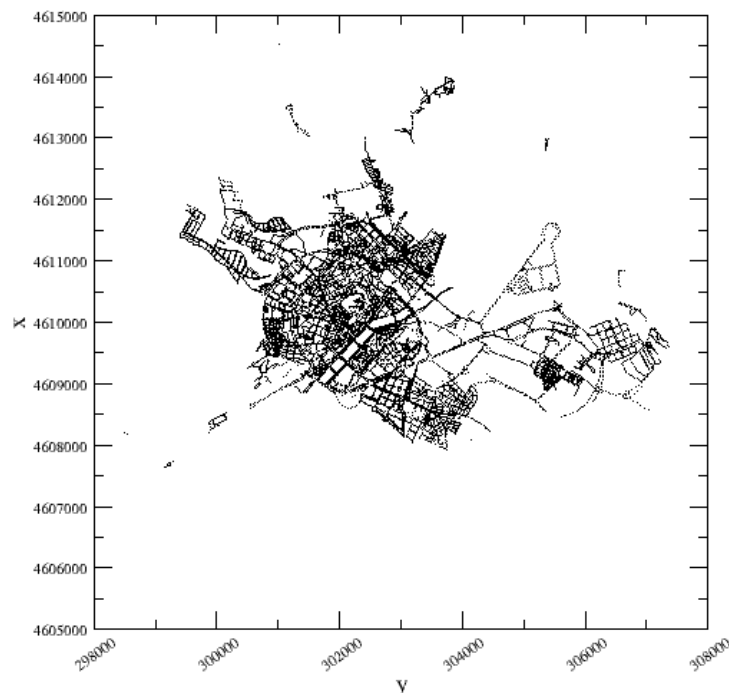


Figure 14. Light sources of Lleida plotted in their provided location

### *Lleida as a light source*

In order to define Lleida as a zone in the way Illumina requires we computed a 3D plot to observe the power concentration in location. As can be seen in figure 15 there is a central zone where most of the power emitted is concentrated and two small concentrations far from the biggest one.

To avoid having an artificially big radius defining Lleida we computed the histogram of the power emitted from the center of Lleida, calculated by averaging the power contribution of each light source. See Figure 16. It will clearly be an error to define the radius of Lleida taking all the lights, because it will be of 20km when most of its power (97.5%) is concentrated within 6km.

Table 2. Difference between cutting in 6km and taking all lights

	All light sources	Central zone	Reduction (%)
Sources	25208	24562	2.5
Radius(m)	20244.38	6576.30	67.5

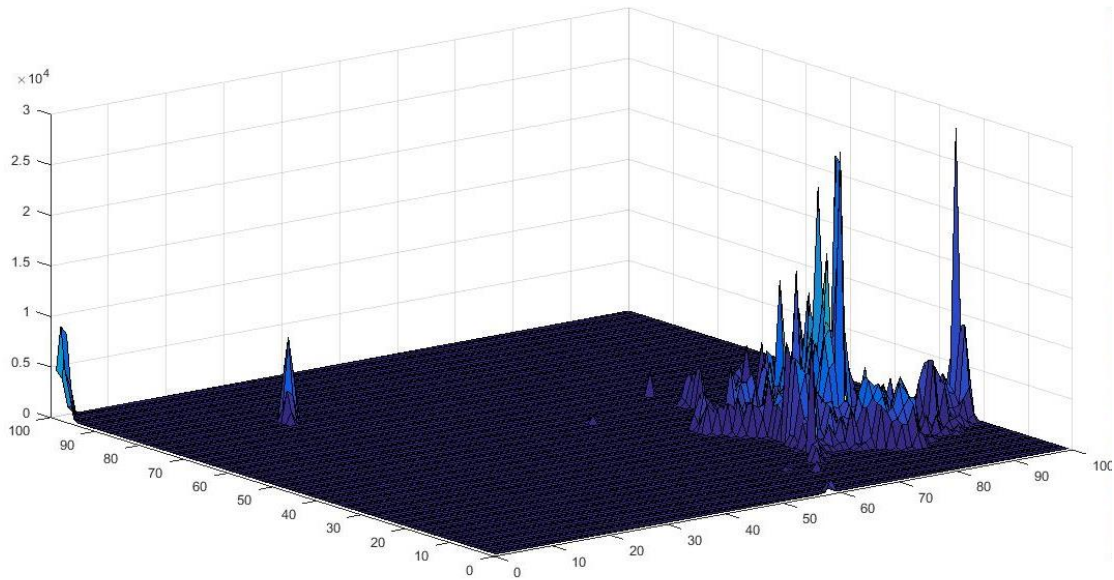


Figure 15. 3D Plot location vs light power emission

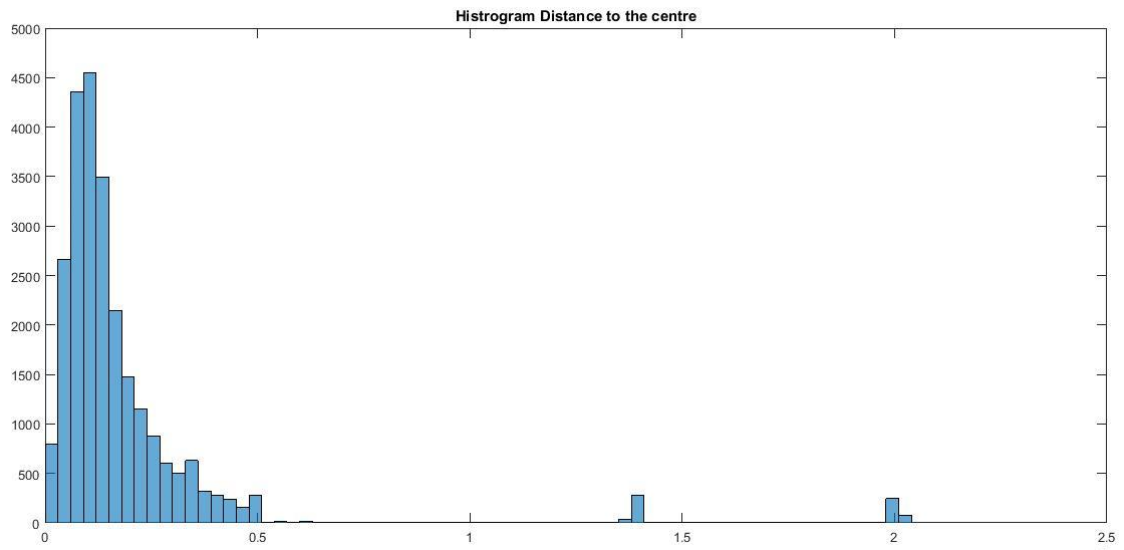


Figure 16. Histogram of light power emission by radial distance to the center

### *Inventory of lights*

There are several kind of lights in both 2014 and 2017 inventories of Lleida. However, in each case there are 3 lamps that add more than 95% of the emitted power (table 3), it is accurate enough though just to take into account the 3 dominant lamps in each case.

The update of the lighting system consisted mostly in replacing all the Mercury Vapor (MV) and some of the Metal Halide (MH) lamps by LEDs. The total number of High Pressure Sodium Vapor (HPSV) is the same in both inventories, the reduction in the percentage is due to a high number of total lights. Although the total number of lights increased the power emission diminished due to higher efficiency of the lamps installed.

It is mandatory to point out that the total power emitted reduction of 33% is not taken into account when performing the computation. The same night light emittance image from 2016 is used for both cases. So the old light emission is actually brighter than the used in the project but it doesn't affect the spectral distribution of the light. In the near future it would be interesting to compute the light pollution produced by the old lights with the correct power.

Table 3. Lleida inventory of lights

	HPSV (%)	MH (%)	LED (%)	MV (%)	Other (%)	#Lamps	Total Power (kW)
2017	65	16	15	0	4	25208	1934.4
2014	71	19	0	7	3	23004	3006.4

Table 4. Percentage of the LOP for each lamp present in the inventory

	2017	2014	2017	2014	2017	2014	2017	2014
<b>ULOR(%)</b>	<b>HPSV (%)</b>		<b>MH (%)</b>		<b>LED (%)</b>		<b>MV (%)</b>	
<b>0</b>	87.5	85.1	98.70	99.66	99.65	-	-	58.94
<b>1</b>	3.98	4.36	0.85	0	0.15	-	-	1.25
<b>5</b>	7.87	9.57	0	0.28	0.06	-	-	32.09
<b>10</b>	0.20	0.11	0.16	0	0	-	-	2.21
<b>50</b>	0.51	0.85	0.24	0.06	0.13	-	-	5.50

Regarding this data, using the format explained in section 2.1.1, the new and the old light inventories of Lleida look like respectively<sup>3</sup>:

15\_4LED\_0 17\_MH\_0 61\_H\_0 7\_H\_10  
19\_MH\_0 62\_H\_0 4\_H\_18\_H\_5 5\_MV\_0 3\_MV\_5

See appendix section for the spectrum and LOP used in the model.

<sup>3</sup> The percentages are not the same than in table 3 because here are weighted to add 100%.

### 3.3. Computation variables

The wavelength range defined has its minimum at 350nm and a maximum at 830nm, and it is divided in 16 windows of 30nm.

The aerosol characterization used corresponds to a rural environment with a relative humidity of 70%. Atmospheric standard pressure (101,3 kPa) and clear sky (no clouds). Typical aerosol optical depth of 0.11, and angstrom coefficients of 0.7.

The dimensions of the region of study, see figure 17, are of 450x400km. Being (0,0) the top-left corner the observer is located at (202, 170) and the center of Lleida at (193,125).

The sky mapping goes from 5° to 90° in elevation with steps of 5°, and covers all the azimuth range with steps of 5° too. This grid results in 19600 lines of sight.



Figure 17. Ground reflectance satellite image of project framework

## 4. Results

The results are displayed with the north upwards and the east rightwards, see figure 18. Elevation angles vary with radius, being the outer one  $5^\circ$  and the center  $90^\circ$ . The analysis of the images presented in 4.1 and 4.2 is done in 4.3.

### 4.1. Apparent magnitudes and colors

In this section you will find first all-sky images in the Johnson's filters B-V-R produced by our tool and measured by ASTMON for both set of lights. At the end, in the same manner, colors produced by directly subtracting the magnitudes computed for two filters are shown.

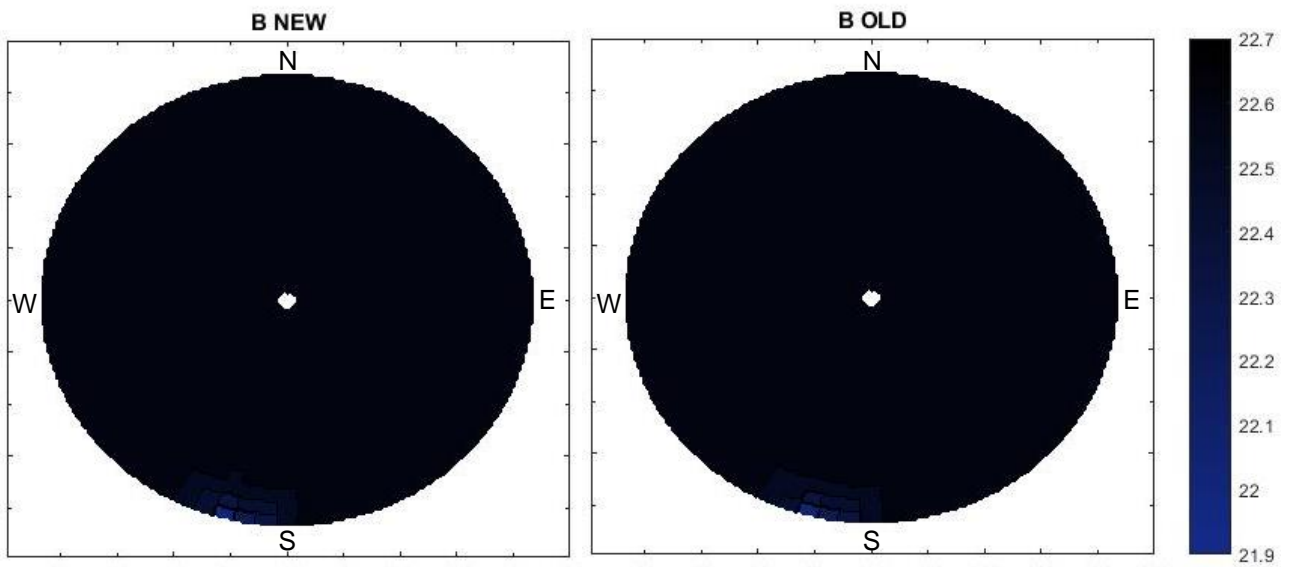


Figure 18. Computed apparent magnitudes in B. Left: new. Right: old

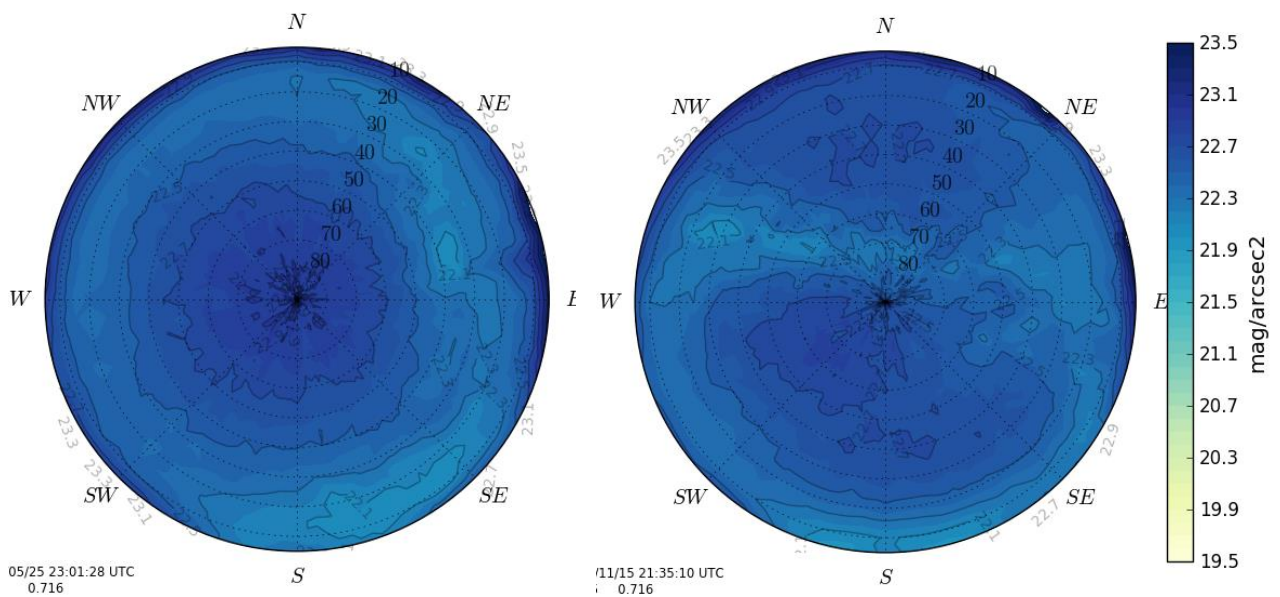


Figure 19. ASTMON measured apparent magnitudes in B. Left: new. Right: old. Processed [13].

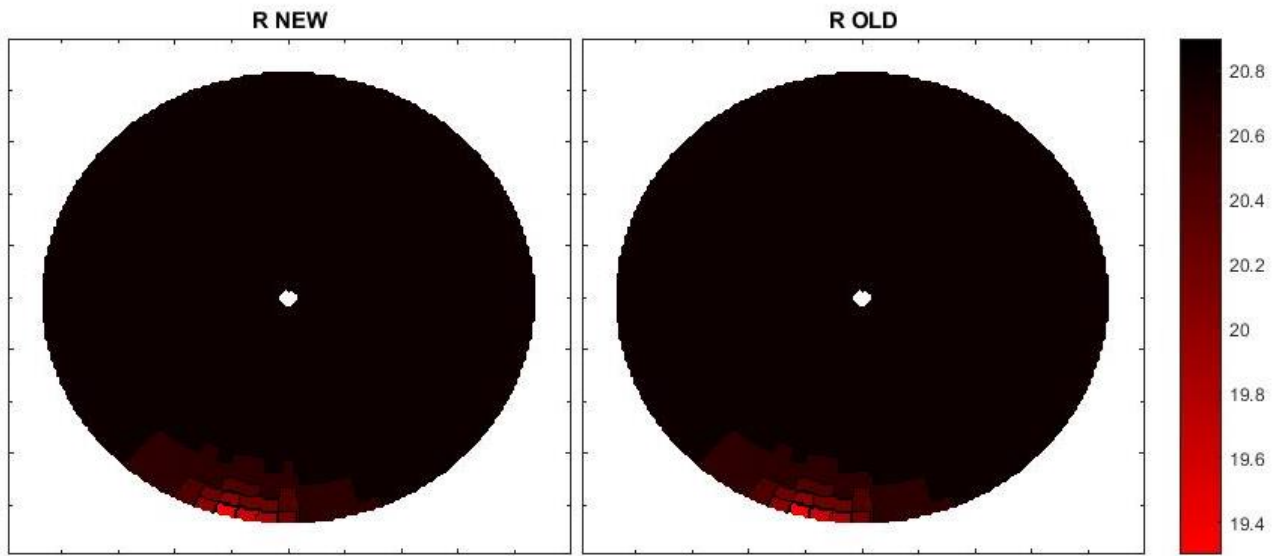


Figure 20. Computed apparent magnitudes in R. Left: new. Right: old

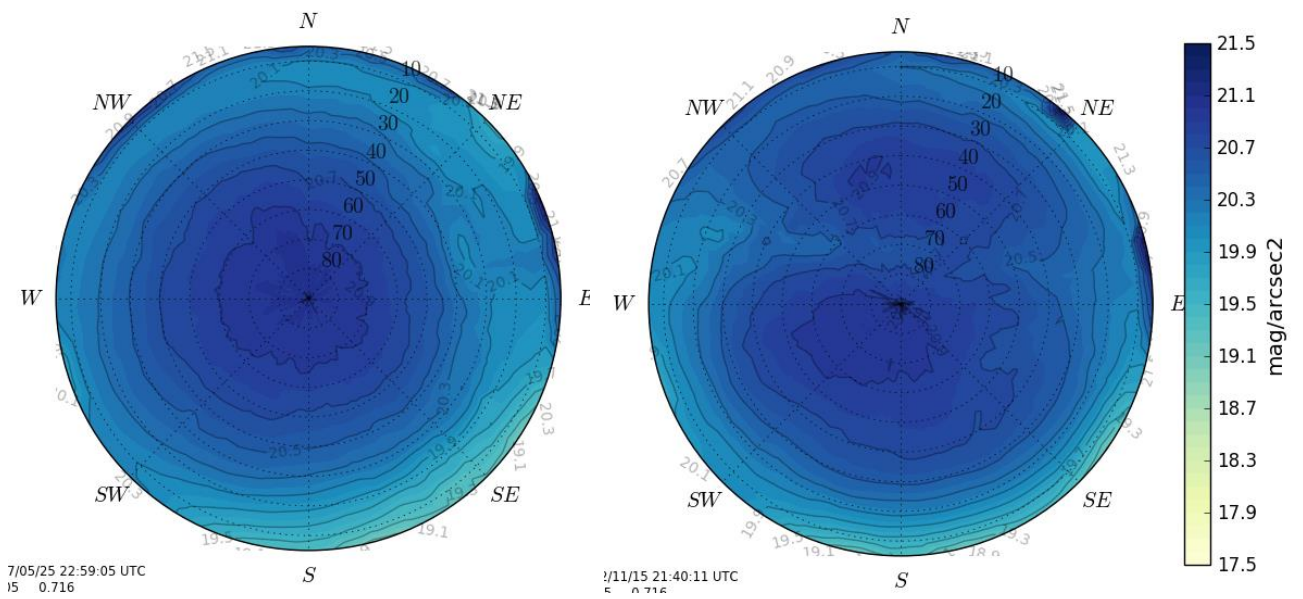


Figure 21. ASTMON measured apparent magnitudes in R. Left: new. Right: old. Processed [13].

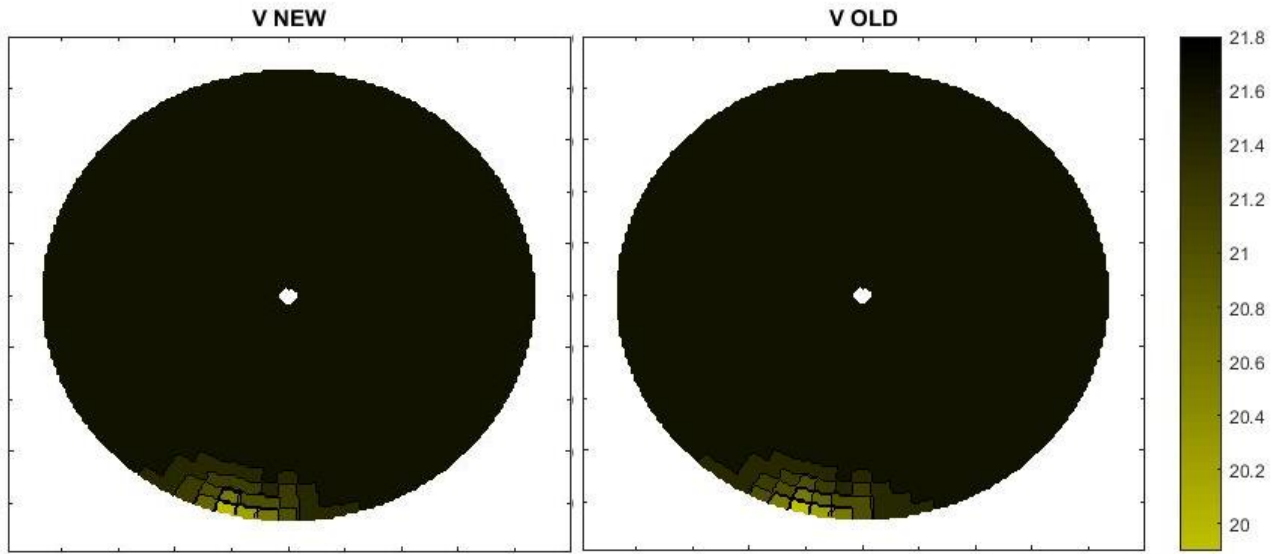


Figure 22. Computed apparent magnitudes in V. Left: new. Right: old

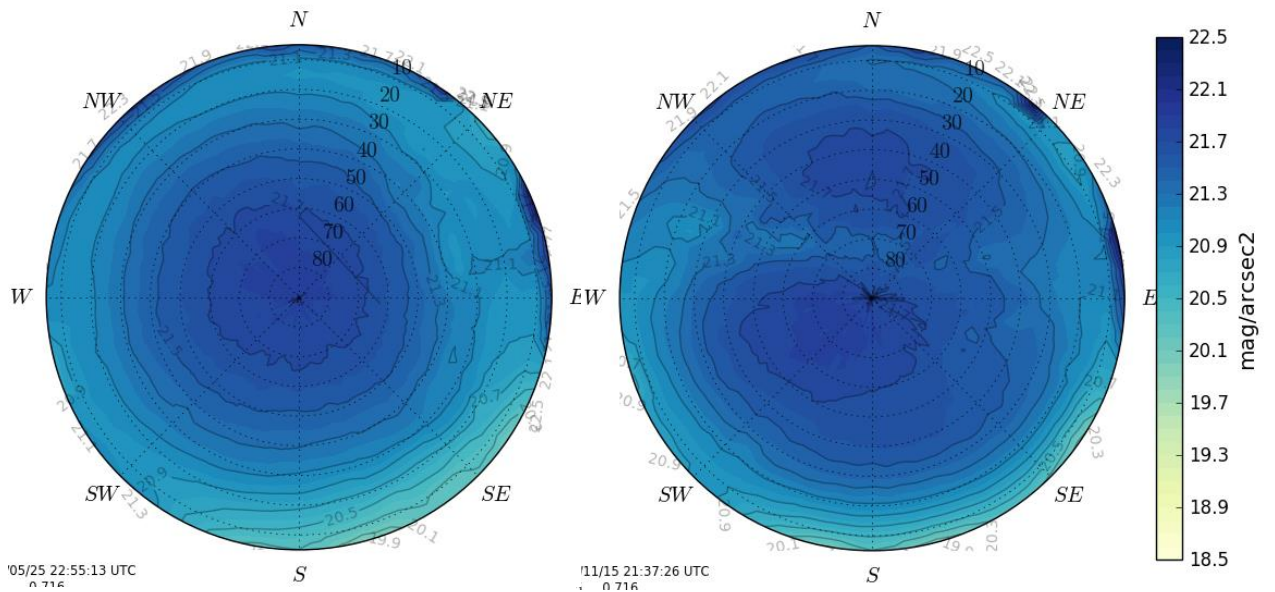


Figure 23. ASTMON measured apparent magnitudes in V. Left: new. Right: old. Processed [13].

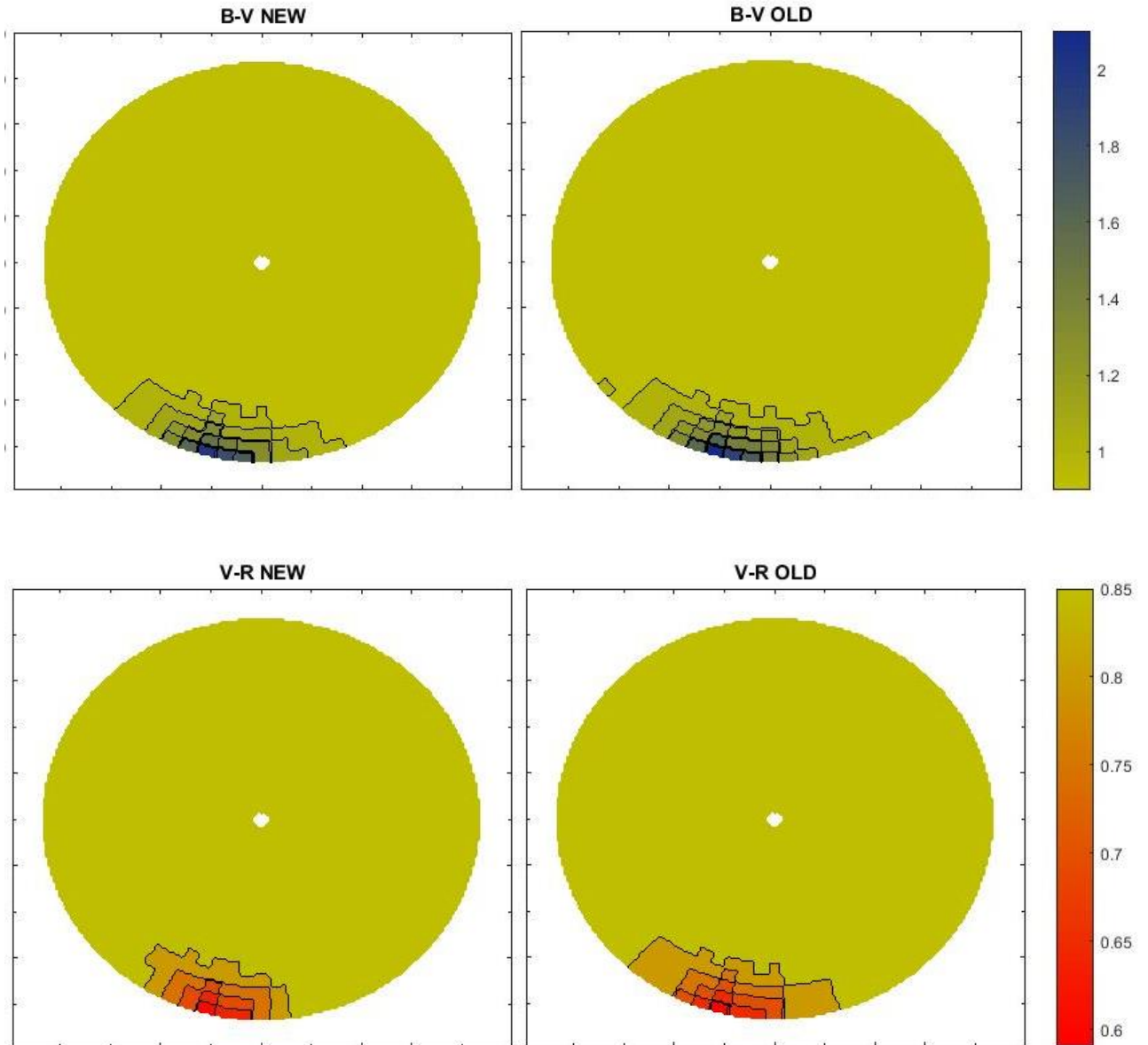


Figure 24. Computed colors.

## 4.2. Comparison between inventories

In this section the result of comparing the spectral flux obtained with Illumina for both scenarios is displayed. This comparison is more accurate than using magnitudes because adding the natural sky brightness and the convolution with the filters could diffuse the results. For the same reason the figures just show the azimuth angle of interest where Lleida is located (145-235°). The equation of the comparison is:

$$C = \frac{F_N - F_O}{F_O} \quad (5)$$

Being  $F_N$  and  $F_O$  the spectral flux of the 2017 and 2014 inventories respectively.

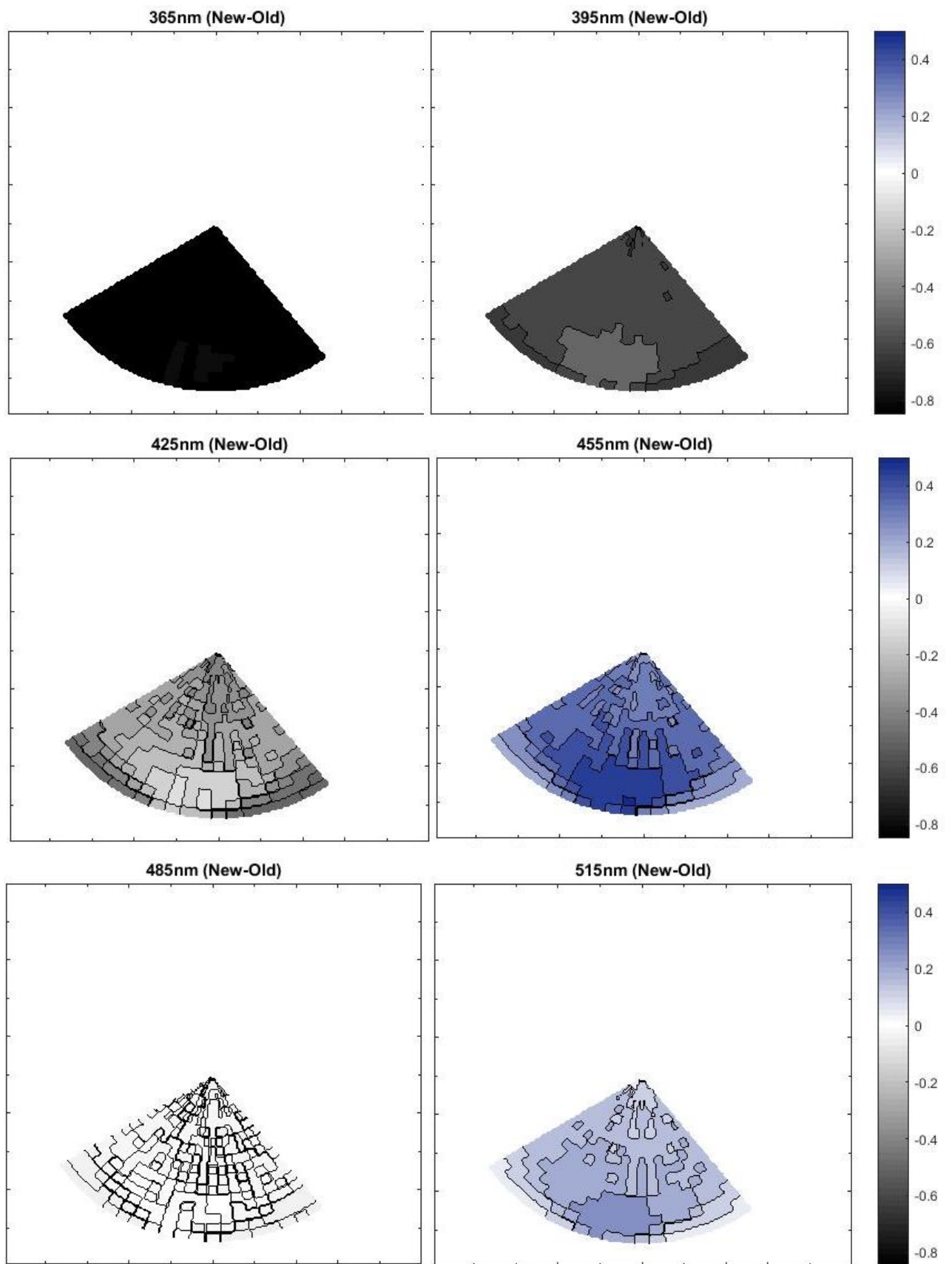


Figure 25. Light-pollution comparison centered at (see header)

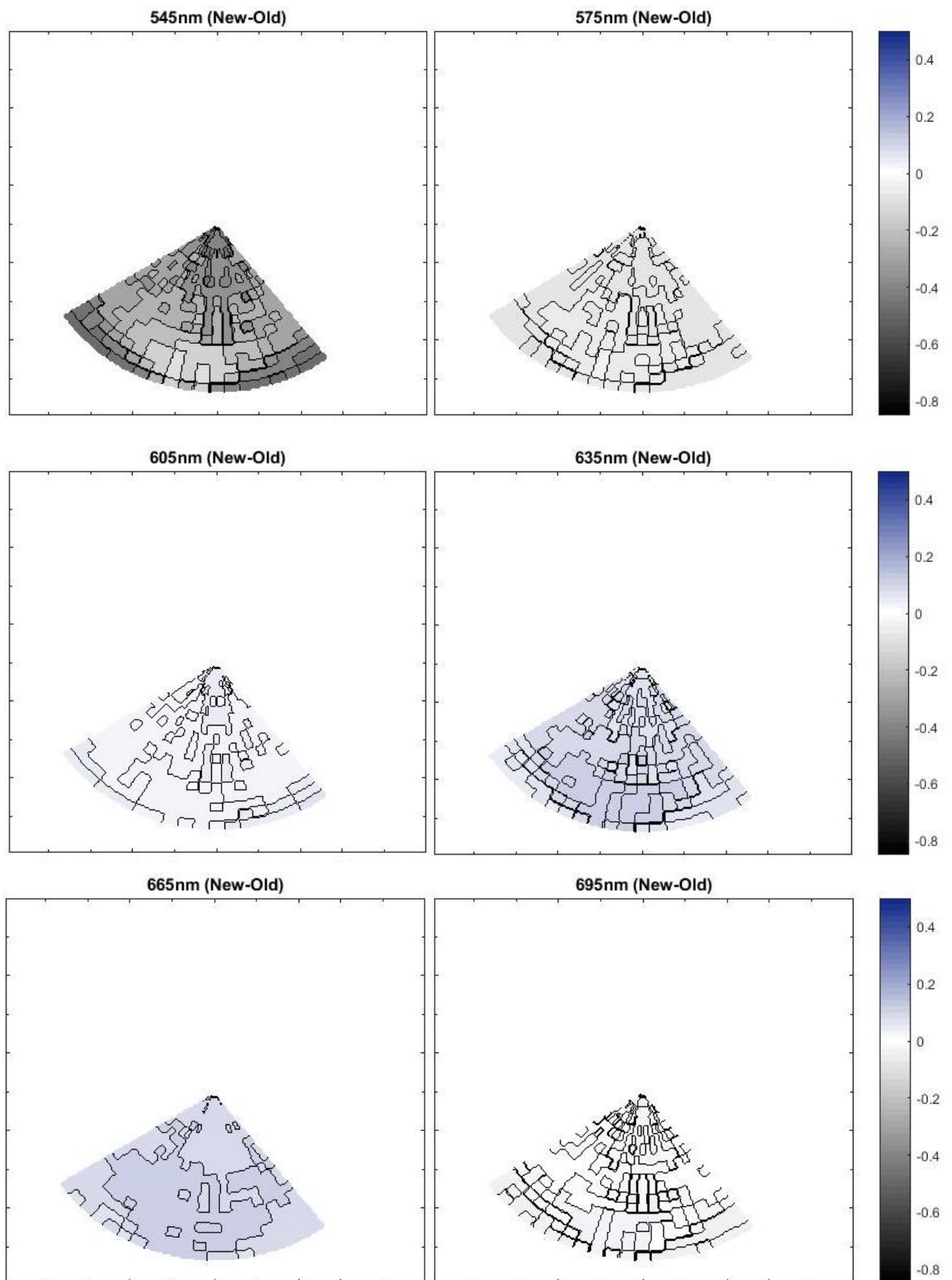


Figure 26. Light-pollution comparison centered at (see header)

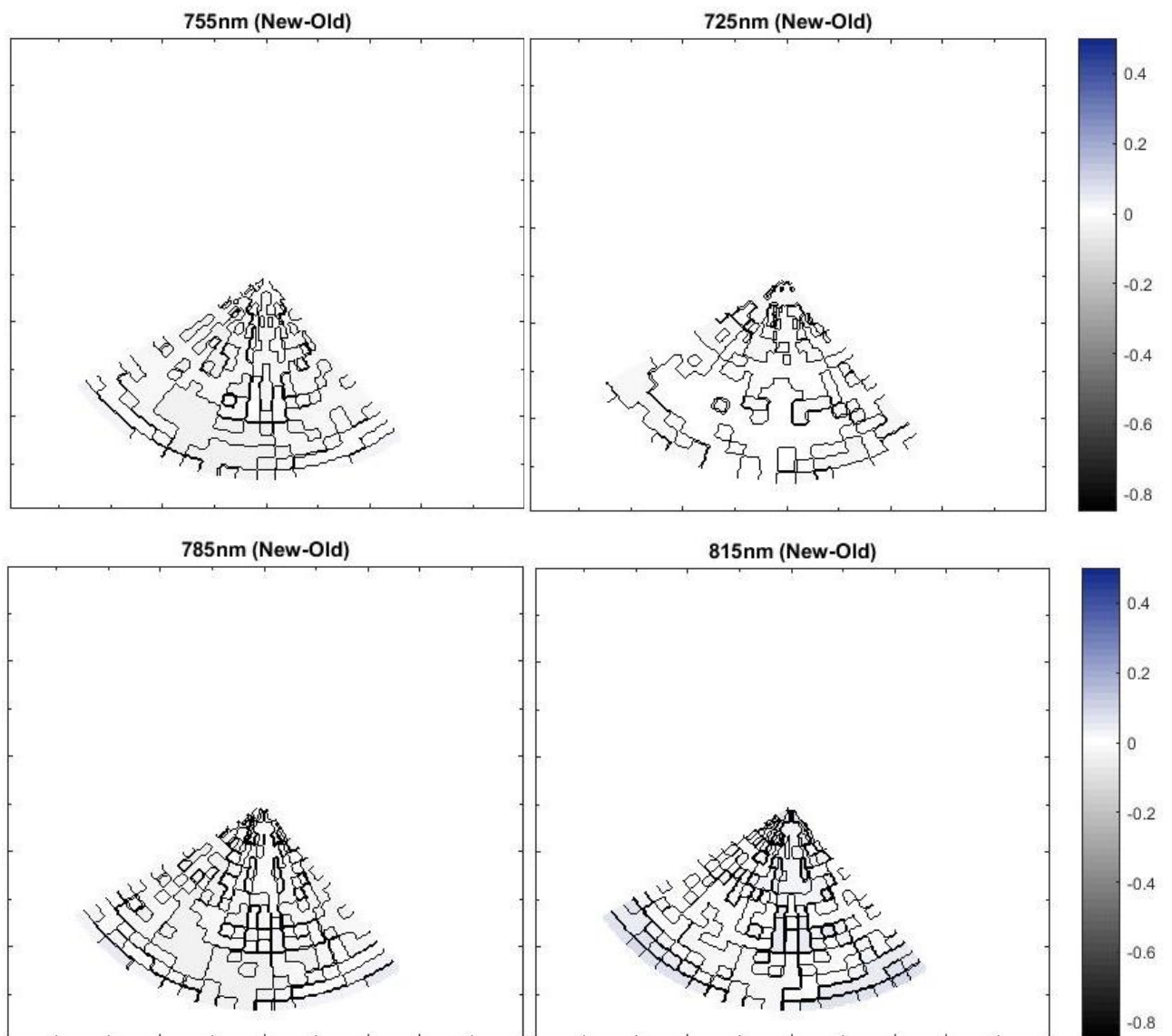


Figure 27. Light-pollution comparison centered at (see header)

### 4.3. Discussion

In 4.1 it's clear that the most affected lines of sight are in the direction of Lleida, 175-205 degrees in azimuth, it is also obvious that the affection is produced in low elevation angles, up to 25 degrees but typically up to 15.

Images from computed light pollution in 4.1 show that light pollution is not uniform among the filters used. In B Lleida enlightens 0.8 magnitudes the natural sky brightness however in R the difference is 1.6 and in V 1.9. The differences in each filter between the old and new inventory are small. Bear in mind we are only accounting for the change in spectrum due to the update in the lighting system, the reduction of power that produced is not taken into account.

Measured images show that Lleida is not the only source of light pollution, there are other directions that point to other light sources such as 120°, which coincides with the direction to Barcelona, and 160° that points to Balaguer, a smaller town than Lleida but much closer. There are other elements that affects the measurement such as the present of the Milky Way. Nevertheless, we can compare the emission in the direction of Lleida at low elevation. Measured and computed light pollution differs slightly but never more than 0.2 magnitudes. In B the measurements are 0.2 fainter than computed, in R 0.2 brighter and in V 0.15 fainter. The intrinsic error in low elevation direction with ASTMON are 0.1 in B and 0.05 in V and R.

The images of colors in 4.1 take into account the natural sky brightness of each filter so the comparison between the two filters is not direct. The difference in color is bigger than in magnitudes. Comparing new and old inventory both in B-V and V-R images we see that the old inventory has a wider emission in the visual than the new one, that could be explained by a reduction of visual light pollution but also with an increment of the blue and/or the red light, another explanation could be a difference in the LOP but the differences of the input are minor.

In 4.2 we tried to find out the different levels of emission in all the visual wavelength range. The images show the comparison between spectral fluxes, a negative number means that the old lights emit more than the new ones and viceversa. Up to 425nm old lights emit much more due to emission of mercury vapor lights present only in the old inventory. At 455nm and 515nm there is much more emission with the new lights (up to 50% more) probably linked with the emission of LED lights. There is a little more emission of the old lights at 545nm due to a peak in the spectrum of mercury vapor. At larger wavelength there are barely no differences, due to the emission is dominated by high pressure sodium vapor and metal halide lights that are present in both inventories.

## 5. Conclusions

The first conclusion is that the methodology to compute the contribution to light pollution from light sources as cities works properly. Lleida has been detected in the coherent azimuth and elevation. The results are coherent with the emission spectrum of the light sources and show a strong relation with them.

Regarding our case of study, Lleida enlightens the sky above Montsec Observatory Park, but the light pollution is confined in a concentrated set of lines of sight around  $190^\circ$  in azimuth and up to  $25^\circ$  in elevation. The light system change that took place in 2014 altered the light emission mostly shifting some emission from the V filter to the B one. As a matter of fact we observe reductions up to 80% in very low wavelength, from 365 to 425nm, and increments up to 50% near the peak of the human scotopic sensitivity at 515nm. It means that a reduction in the energy consumed by light sources doesn't necessarily mean a reduction in the amount of light emitted in the whole spectrum.<sup>4</sup> Even if it seems to naked eye that there has been a reduction in emission it could have just only shifted to wavelengths not as sensitive to the visual but as much troublesome for astronomers and even more harmful for human health. Simplifications as not taking into account natural sources of light, such as the Milky Way, and other cities around the observer make it difficult to compare the results with measured all-sky ASTMON data. But measurements in the lines of sights affected by Lleida agrees in order of magnitude with the results.

In the near future in order to have a more accurate look into light pollution in the PAM we are working in getting the inventory of lights of Balaguer to add it as a light source. We are also on the run to obtain the satellite night light emittance images of Lleida previous to the update in the lighting system. Middle-term objectives should focus on combining the light emittance input that uses Illumina from satellite data with public inventories because the former takes into account all lights, public or private, and the second one is more accurate with the public ones.

This methodology can be used easily as a first overall estimation of light pollution affectation with relatively low accurate inventory of lights and conditions. To perform more specific studies in which certain wavelength must be studied carefully the user have to bear in mind to obtain an almost perfect spectrum of the lights studied.

This project was a first trial working with Illumina, in the light of the results obtained and the offered collaboration from institutions it could be a starting point for studying other areas of interest in Catalonia.

---

<sup>4</sup> The reduction in power emitted was 33% so even taking it into account the emission at 515nm will be greater in 2017.

## References

- [1] Martin Aubé et al. "Wikipedia de Martin Aubé: Illumina Project".  
<http://cegepssherbrooke.qc.ca/~aubema/index.php/Prof/IllumEn>
- [2] International Dark Sky Association. <http://www.darksky.org/>
- [3] NASA Blue Marble Navigator. <https://blue-marble.de/nightlights/2012>
- [4] Martin Aubé, "Improved light pollution models allow the simulation of real situations", SPIE Astronomy, 2006
- [5] PAM official website: <http://www.parcastroomic.cat/>
- [6] Aubé, Martin. "Light pollution modeling and detection in a heterogeneous environment." Proceedings of Starlight 2007 conference, La Palma, Spain. 2007.
- [7] Aceituno, Jesús, et al. "An all-sky transmission monitor: ASTMON." Publications of the Astronomical Society of the Pacific 123.907 (2011): 1076.
- [8] Longcore, T. & Rich, C. 2004. *Frontiers in Ecology and the Environment* 2(4), 191.
- [9] Hölker, F. et al 2010. *Ecology and Society*, 15, 1.
- [10] Fabio Falchi, Pierantonio Cinzano, Dan Duriscoe, Christopher C. M. Kyba, Christopher D. Elvidge, Kimberly Baugh, Boris A. Portnov, Nataliya A. Rybnikova, Riccardo Furgoni. "The new world atlas of artificial night sky brightness." *Science Advances* 10 Jun 2016: vol. 2, no. 6.
- [11] Simoneau, Alexandre. "Modélisation de la radiance artificielle du ciel nocturne à Hawaï et élaboration d'un plan de restauration optimisé du ciel étoilé." Résumé (2016).
- [12] Illumina users guide. Martin et al.  
<http://cegepssherbrooke.qc.ca/~aubema/index.php/Prof/IlluminaGuide2016>
- [13] Post-process of ASTMON data.  
pyASB (Nievas, M.. Absolute photometry and sky brightness with astmon-ucm. Master's thesis; Universidad Complutense de Madrid; 2013.)
- [14] Night sky brightness: <https://www.astro.umd.edu/~ssm/ASTR620/mags.html>  
Source NOAO Newsletter #10.
- [15] Kurucz, R.L. (2005). "AtLAS12, SYNTHE, ATLAS9, WIFTH9, etcera". *Memorie della Societa Astronomica Italiana supplementi* 8, p. 14.

## Appendix

### A.1. Spectrum of lamps used in the model

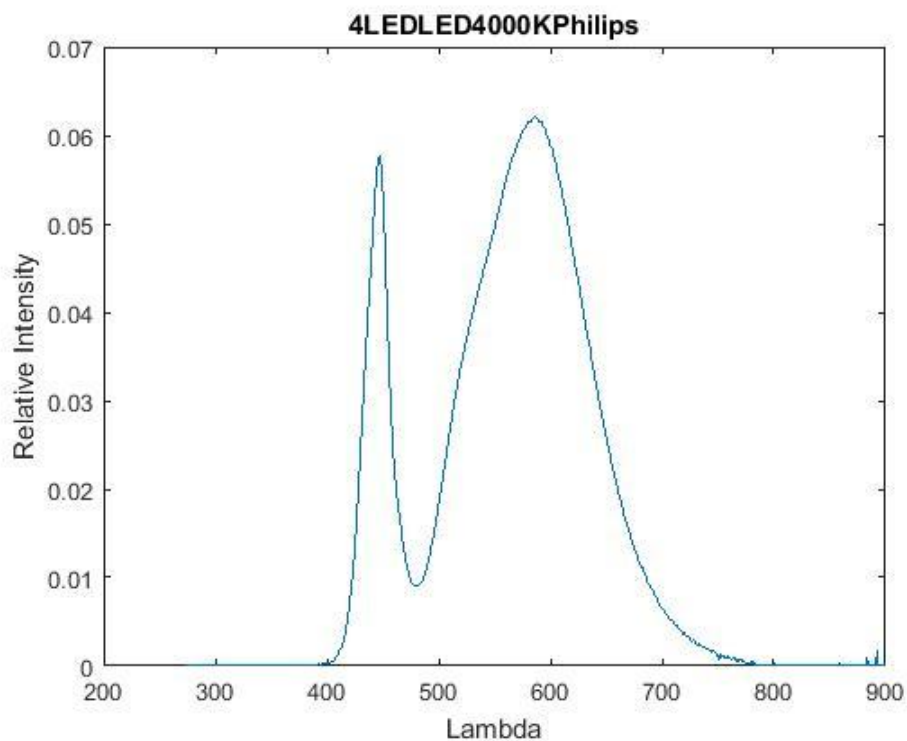


Figure 28. Spectrum of LEDs at 4000K

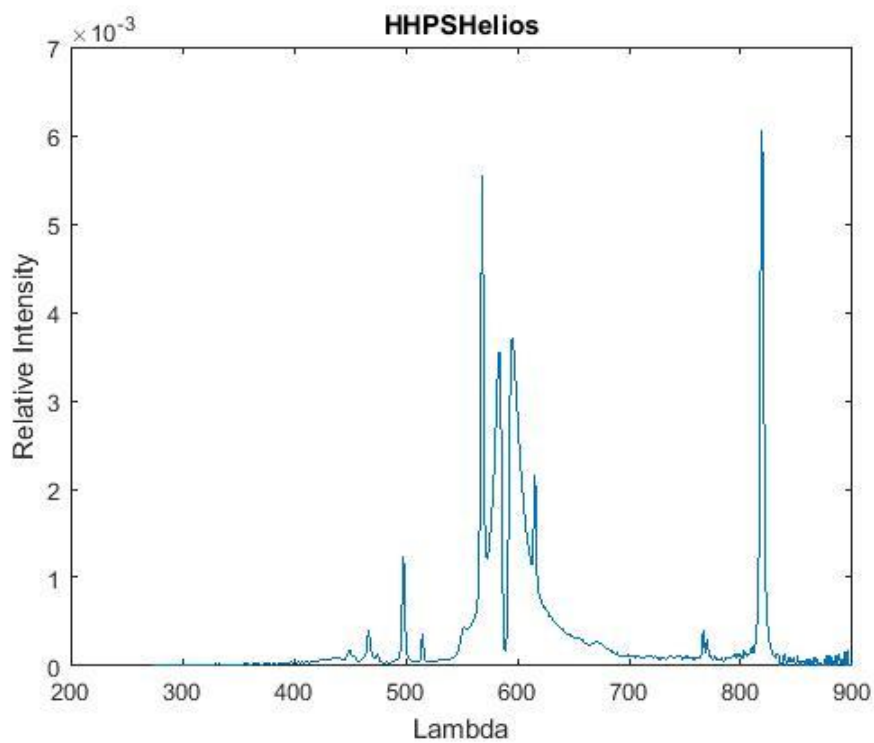


Figure 29. Spectrum of HPSV

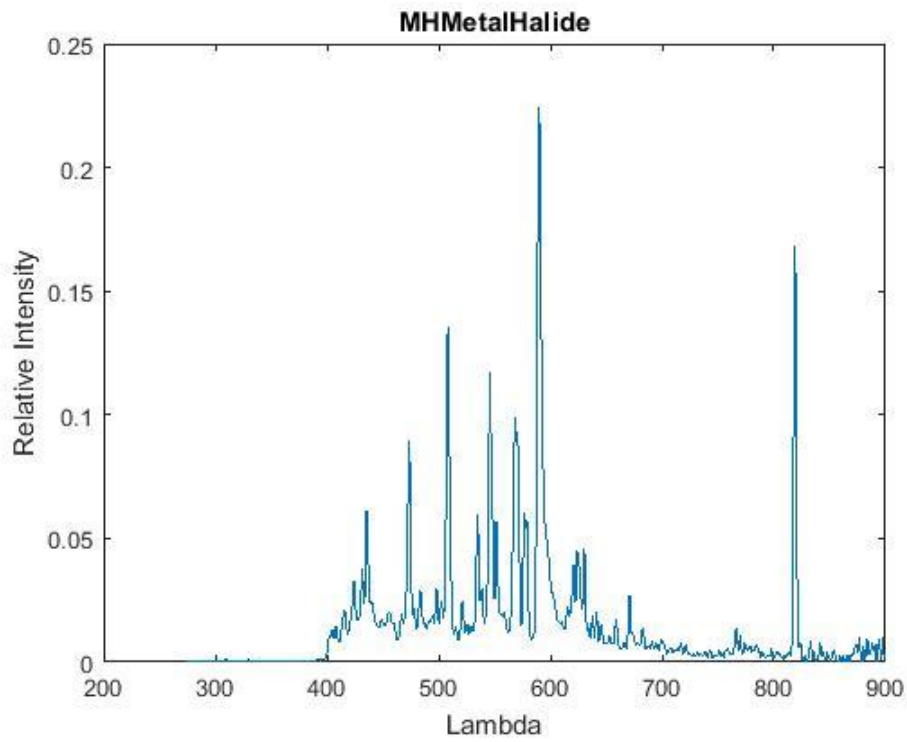


Figure 30. Spectrum of Metal Halide

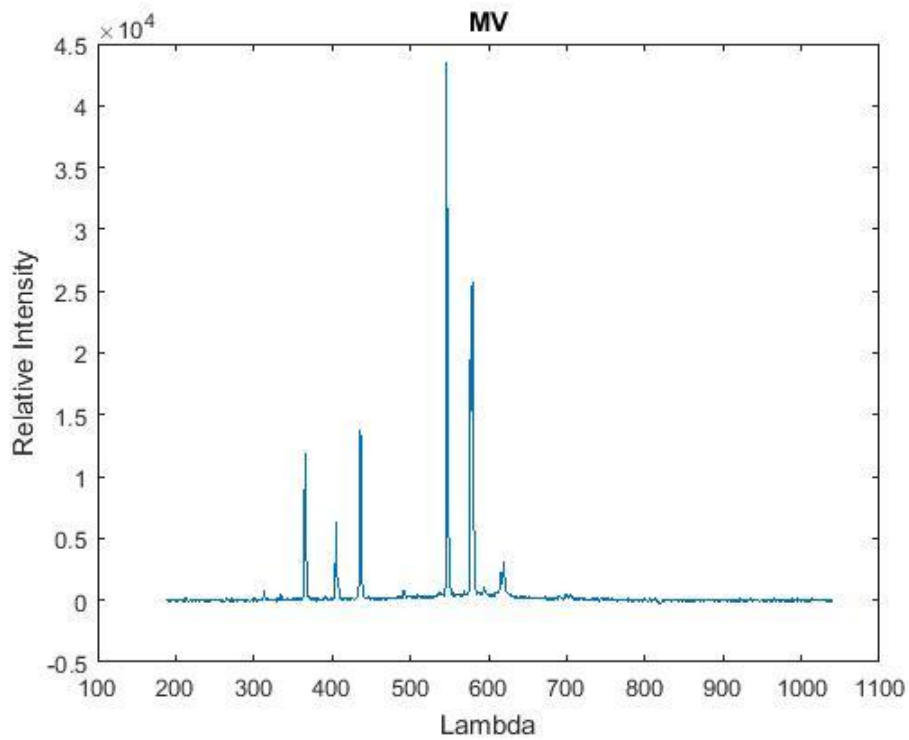


Figure 31. Spectrum of MV

## A.2. LOP used of the lighting system used in the model

In the following plot  $0^\circ$  points to the zenith and  $180^\circ$  to the ground.

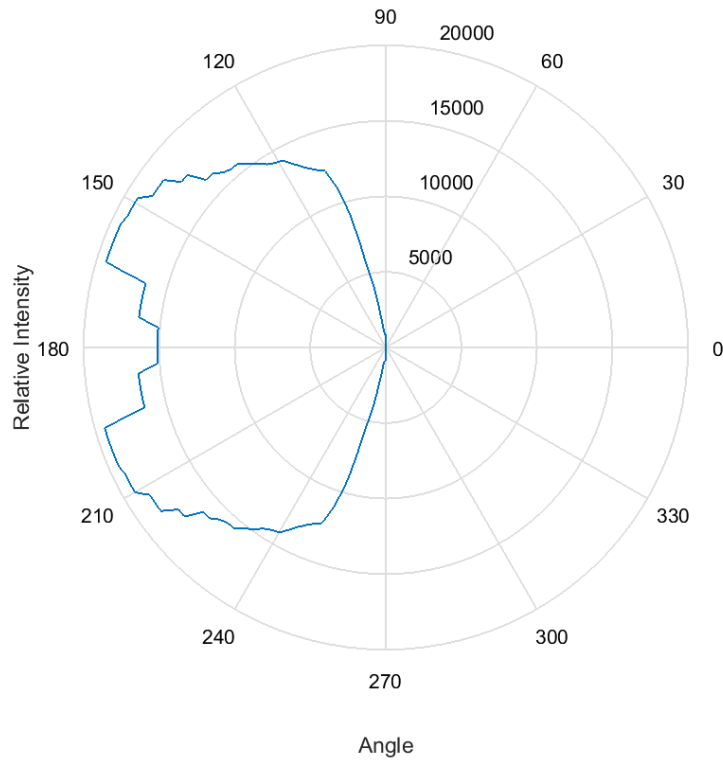


Figure 32. LOP of 0% FHS

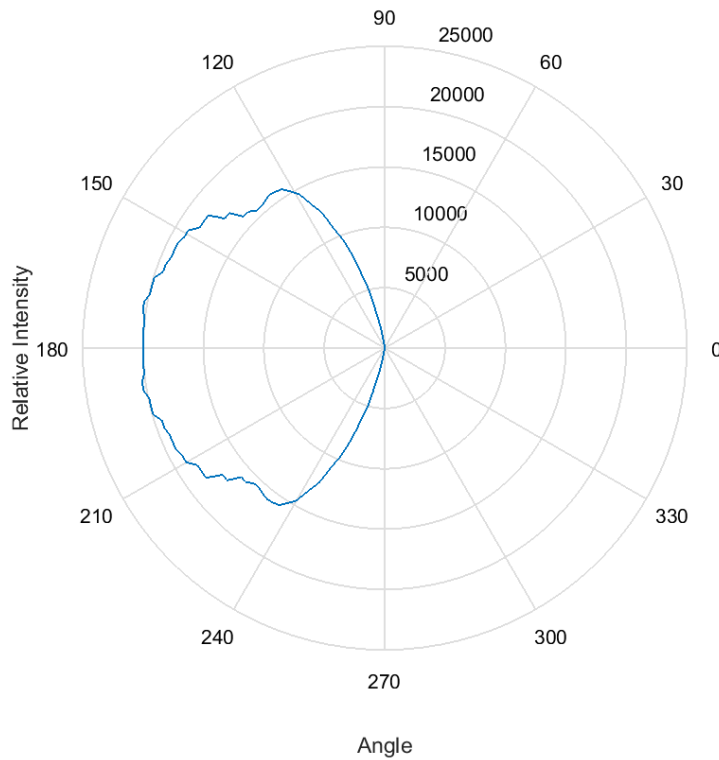


Figure 33. LOP of 1% FHS

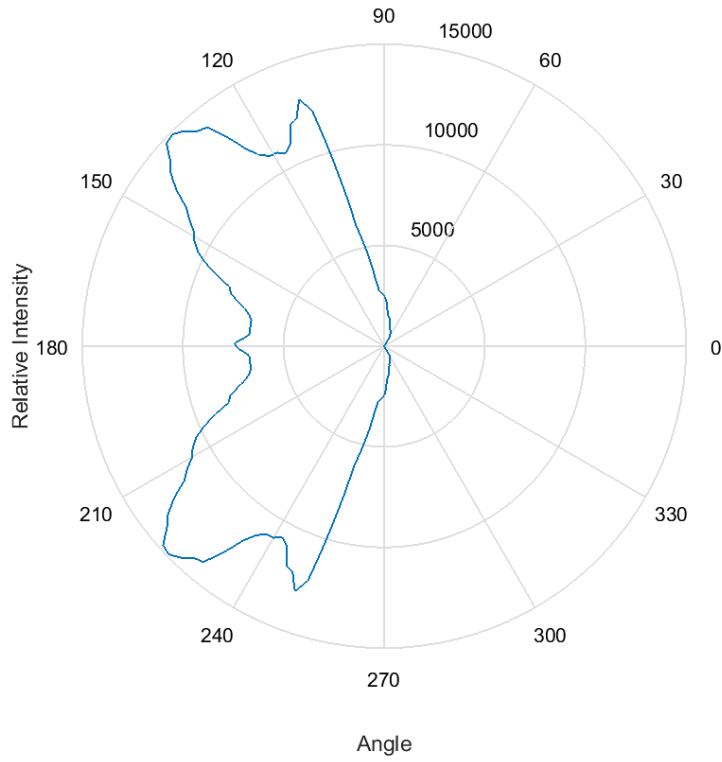


Figure 34. LOP of 5% FHS

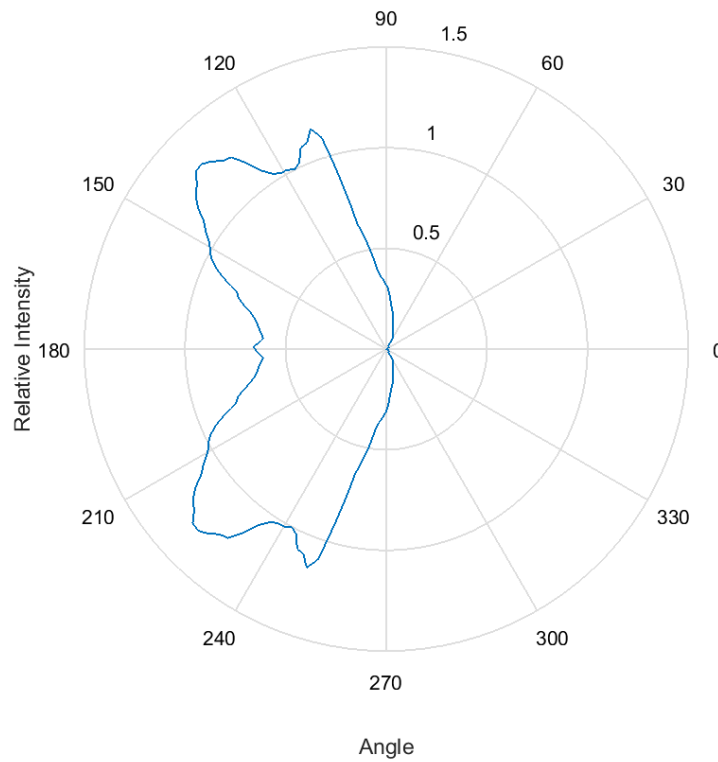


Figure 35. LOP of 10% FHS

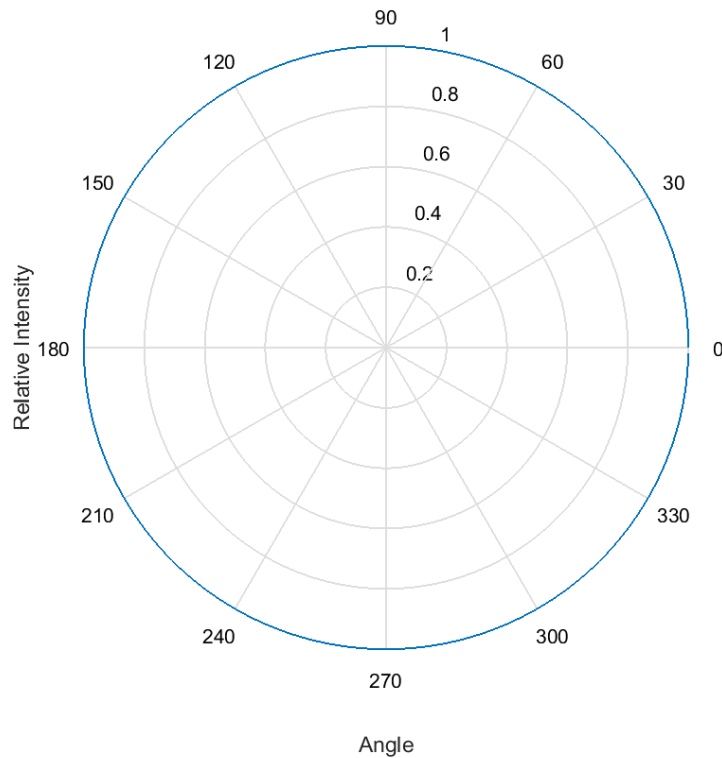


Figure 36. LOP of 50% FHS

## A.3. Post-processing code

### A.3.1. Main

```

%% Loading the required data: output of illumina for new and old
inventory,
%filter functions, vega flux function with wavelength
data=load('data_new.txt');
data2=load('data_old.txt');
filtb=load('filtB.dat');
filtv=load('filtV.dat');
filtr=load('filtR.dat');
vega=load('alpha_lyr_mod_002.dat');
%% Function for smoothin to steps of 1nm the johnson's filter
[fb, fv, fr]=filtres1nm(filtb, filtv, filtr);

%% Computing the flux of Vega inV, B and R

str=pi/(180^2*3600^2); %conversion factor between str and arcsec^2
for i=1:910
    [miny, position]=min(abs(vega(:,2)-i));
    if((i-0.5)<fb(1,1) || (i+0.5)>fb(end,1))
        vegab(i)=0;
    else
        a2=find(fb(:,1)<(i+0.5) & fb(:,1)>=(i-0.5));
        vegab(i)=fb(a2,2)*vega(position,4);
    end
    if((i-0.5)<fv(1,1) || (i+0.5)>fv(end,1))
        vegav(i)=0;
    else

```

```

        a2=find(fv(:,1)<(i+0.5) & fv(:,1)>=(i-0.5));
        vegav(i)=fv(a2,2)*vega(position,4);
    end
    if((i-0.5)<fr(1,1) || (i+0.5)>fr(end,1))
        vegar(i)=0;
    else
        a2=find(fr(:,1)<(i+0.5) & fr(:,1)>=(i-0.5));
        vegar(i)=fr(a2,2)*vega(position,4);
    end
end

end

% Integral filtre v
% f= can be either an anonymous function (e.g. f=@(x) sin(x)) or a
vector
% containing equally spaced values of the function to be integrated
% a= Initial point of interval
% b= Last point of interval
% n= # of sub-intervals (panels), must be integer
% I= h/3*(f(1)+2*sum(f(3:2:end-2))+4*sum(f(2:2:end))+f(end));
nv=numel(vegav)-1; hv=(fv(end,1)-fv(1,1))/nv;
nr=numel(vegar)-1; hr=(fr(end,1)-fr(1,1))/nr;
nb=numel(vegab)-1; hb=(fb(end,1)-fb(1,1))/nb;

FVV=hv/3*(vegav(1)+2*sum(vegav(3:2:end-
2))+4*sum(vegav(2:2:end))+vegav(end));
FVR=hr/3*(vegar(1)+2*sum(vegar(3:2:end-
2))+4*sum(vegar(2:2:end))+vegar(end));
FVB=hb/3*(vegab(1)+2*sum(vegab(3:2:end-
2))+4*sum(vegab(2:2:end))+vegab(end));

% Computing the flux of the natural sky brightness
brcnB=FVB*10^(0.4*(-0.023-22.7));
brcnV=FVV*10^(0.4*(-0.023-21.8));
brcnR=FVR*10^(0.4*(-0.023-20.9));

% Apparent magnitudes in B-V-R of the light pollution
%New inventory
for el=5:5:90
    if el==90
        azlim=0;
    else
        azlim=355;
    end
    for az=0:5:azlim
        a=find(data(:,2)==el & data(:,3)==az); %%trobem els index
d'una direccio i totes les lambdes
        %Filling the array for steps of 1nm

        %option a) same value for the whole window

        for j=1:size(a,1)
            for i=1:910
                if (data(a(j,1),1)>i-15 && data(a(j,1),1)<=i+15)
                    lm(i)=data(a(j,1),4)/30;%El 30 es per tenir
unitats w/m2/nm
                end
            end
        end
    end
end
end
end

```

```

window
    %option b) interpolation taken as data the center of the
    [lm]=illumina1nm(data,a,el,az);

    %Multiply filter and light pollution function
    for i=1:910
        if((i-0.5)<fb(1,1) || (i+0.5)>fb(end,1))
            mb(i)=0;
        else
            a2=find(fb(:,1)<i+0.5 & fb(:,1)>=i-0.5);
            mb(i)=lm(i)*fb(a2,2);
        end
        if((i-0.5)<fv(1,1) || (i+0.5)>fv(end,1))
            mv(i)=0;
        else
            a2=find(fv(:,1)<i+0.5 & fv(:,1)>=i-0.5);
            mv(i)=lm(i)*fv(a2,2);
        end
        if((i-0.5)<fr(1,1) || (i+0.5)>fr(end,1) || i>829)
            mr(i)=0;
        else
            a2=find(fr(:,1)<i+0.5 & fr(:,1)>=i-0.5);
            mr(i)=lm(i)*fr(a2,2);
        end
    end

    %integral of the resulting function
    nmv=numel(mv)-1; hmv=(fv(end,1)-fv(1,1))/nmv;
    nmr=numel(mr)-1; hmr=(fr(end,1)-fr(1,1))/nmr;
    nmb=numel(mb)-1; hmb=(fb(end,1)-fb(1,1))/nmb;

    FMV=hmv/3*(mv(1)+2*sum(mv(3:2:end-
2))+4*sum(mv(2:2:end))+mv(end));
    FMR=hmr/3*(mr(1)+2*sum(mr(3:2:end-
2))+4*sum(mr(2:2:end))+mr(end));
    FMB=hmb/3*(mb(1)+2*sum(mb(3:2:end-
2))+4*sum(mb(2:2:end))+mb(end));

    %Computing the apparent magnitudes for each direction
    MMVN(el,az+1)=-0.023-2.5*log10((FMV*str+brcnV)/FVV);
    MMBN(el,az+1)=-0.023-2.5*log10((FMB*str+brcnB)/FVB);
    MMRN(el,az+1)=-0.023-2.5*log10((FMR*str+brcnR)/FVR);
end

end

%old inventory
for el=5:5:90
    if el==90
        azlim=0;
    else
        azlim=355;
    end
    for az=0:5:azlim
        a3=find(data2(:,2)==el & data2(:,3)==az); %%trobem els index
d'una direccio i totes les lambdes
        % a) same value all the window
        for j=1:size(a,1)
            for i=1:910
                if (data2(a(j,1),1)>i-15 && data2(a(j,1),1)<=i+15)

```

```

%                               lm(i)=data2(a(j,1),4)/30;%El 30 es per tenir
unitats w/m2/nm
%                               end
%                               end
%                               end
%option b) interpolation
[lm]=illumina1nm(data2,a3,e1,az);

for i=1:910
    if((i-0.5)<fb(1,1) || (i+0.5)>fb(end,1))
        mb(i)=0;
    else
        a4=find(fb(:,1)<i+0.5 & fb(:,1)>=i-0.5);
        mb(i)=lm(i)*fb(a4,2);
    end
    if((i-0.5)<fv(1,1) || (i+0.5)>fv(end,1))
        mv(i)=0;
    else
        a4=find(fv(:,1)<i+0.5 & fv(:,1)>=i-0.5);
        mv(i)=lm(i)*fv(a4,2);
    end
    if((i-0.5)<fr(1,1) || (i+0.5)>fr(end,1) || i>829)
        mr(i)=0;
    else
        a4=find(fr(:,1)<i+0.5 & fr(:,1)>=i-0.5);
        mr(i)=lm(i)*fr(a4,2);
    end
end

nmv=numel(mv)-1; hmv=(fv(end,1)-fv(1,1))/nmv;
nmr=numel(mr)-1; hmr=(fr(end,1)-fr(1,1))/nmr;
nmb=numel(mb)-1; hmb=(fb(end,1)-fb(1,1))/nmb;

FMV=hmv/3*(mv(1)+2*sum(mv(3:2:end-
2))+4*sum(mv(2:2:end))+mv(end));
FMR=hmr/3*(mr(1)+2*sum(mr(3:2:end-
2))+4*sum(mr(2:2:end))+mr(end));
FMB=hmb/3*(mb(1)+2*sum(mb(3:2:end-
2))+4*sum(mb(2:2:end))+mb(end));

MMVO(e1,az+1)=-0.023-2.5*log10((FMV*str+brcnV)/FVV);
MMBO(e1,az+1)=-0.023-2.5*log10((FMB*str+brcnB)/FVB);
MMRO(e1,az+1)=-0.023-2.5*log10((FMR*str+brcnR)/FVR);
end

end

%% Computing Colors
BVN=MMBN-MMVN;
VRN=MMVN-MMRN;
BVO=MMBO-MMVO;
VRO=MMVO-MMRO;

%% Displaying the output
contourv3(MMRN, MMBN, MMVN, BVN, VRN)
contourv3(MMRO, MMBO, MMVO, BVO, VRO)

```

### A.3.2. Johnson filter smoothing function

`% Function to smooth the Johnson's filter function to step of 1nm`

```
function [fb, fv, fr]=filtres1nm(filtb, filt v, filtr)
cont=0;
cont2=0;
for i=filtb(1,1):filtb(end,1)
    cont=cont+1;
    fb(cont,1)=i;
    if mod(i,10)==0
        cont2=cont2+1;
        fb(cont,2)=(filtb(cont2,2));
    else
        fb(cont,2)=(filtb(cont2+1,2)-
filtb(cont2,2))/(filtb(cont2+1,1)-filtb(cont2,1))*(i-
filtb(cont2,1))+filtb(cont2,2);
    end
end
cont=0;
cont2=0;
for i=filtv(1,1):filtv(end,1)
    cont=cont+1;
    fv(cont,1)=i;
    if mod(i,10)==0
        cont2=cont2+1;
        fv(cont,2)=(filtv(cont2,2));
    else
        fv(cont,2)=(filtv(cont2+1,2)-
filtv(cont2,2))/(filtv(cont2+1,1)-filtv(cont2,1))*(i-
filtv(cont2,1))+filtv(cont2,2);
    end
end
cont=0;
cont2=0;
for i=filtr(1,1):filtr(end,1)
    cont=cont+1;
    fr(cont,1)=i;
    if mod(i,10)==0
        cont2=cont2+1;
        fr(cont,2)=(filtr(cont2,2));
    else
        fr(cont,2)=(filtr(cont2+1,2)-
filtr(cont2,2))/(filtr(cont2+1,1)-filtr(cont2,1))*(i-
filtr(cont2,1))+filtr(cont2,2);
    end
end
```

### A.3.3. Illumina output smooth

`%Obtaining values for each nm interpolating between window centers`

```
function [lm2]=illumina1nm(data,a,e1,az)
%Sort the wl
for l=1:size(a,1)
    for j=1:size(a,1)-1
        if data(a(j,1),1)>data(a(j+1,1),1)
            temp=data(a(j,1),:);
            data(a(j,1),:)=data(a(j+1,1),:);
            data(a(j+1,1),:)=temp;
        else
```

```

        temp=0;
    end
end
end
%Smoothing
cont=0;
for i=350:830
    if size(a,1)==0
        lm2(i)=0;
    else
        if i==365+cont*30
            cont=cont+1;
            b=find(data(:,1)==i & el==data(:,2) & az==data(:,3));
            lm2(i)=data(b(1),4)/30;
        else
            if i<365
                lm2(i)=(((data(a(1,1),4))/(data(a(1,1),1)-350))*(i-
350))/30;
            elseif i>815
                lm2(i)=((-data(a(end,1),4))/(830-
data(a(end,1),1)))*(i-data(a(end,1),1)+data(a(end,1),4))/30;
            else
                lm2(i)=(((data(a(cont+1,1),4)-
data(a(cont,1),4))/(data(a(cont+1,1),1)-data(a(cont,1),1)))*(i-
data(a(cont,1),1))+data(a(cont,1),4))/30;
            end
        end
    end
end
end
end

```

### A.3.4. Displaying results in polar plot with concentric circles for elevation

```

function []=contourv3(MMRN, MMBN, MMVN, BVN, VRN)
matrixr=zeros(200,200);
matrixb=zeros(200,200);
matrixv=zeros(200,200);
matrixc1=zeros(200,200);
matrixc2=zeros(200,200);
for j=90:-5:5
    n=90-j;
    for i=1:5:356
        for k=1:200
            for m=1:200
                angy=m-100;
                angx=k-100;
                if(sqrt(angx^2+angy^2)>(n-2.5) &&
sqrt(angx^2+angy^2)<(n+2.5))
                    if j==90
                        matrixr(k,m)=MMRN(j,i);
                        matrixb(k,m)=MMBN(j,i);
                        matrixv(k,m)=MMVN(j,i);
                        matrixc1(k,m)=BVN(j,i);
                        matrixc2(k,m)=VRN(j,i);
                    else
                        ang=atand(angy/angx);
                        if angx>=0 && angy>=0
                            if (ang>((i-1)-2.5) && ang<((i-1))+2.5)
                                matrixr(k,m)=MMRN(j,i);
                            end
                        end
                    end
                end
            end
        end
    end
end

```

```

        matrixb(k,m)=MMBN(j,i);
        matrixv(k,m)=MMVN(j,i);
        matrixc1(k,m)=BVN(j,i);
        matrixc2(k,m)=VRN(j,i);
    end
elseif angx>=0 && angy<0
    ang=ang+360;
    if (ang>((i-1)-2.5) && ang<((i-1)+2.5))
        matrixr(k,m)=MMRN(j,i);
        matrixb(k,m)=MMBN(j,i);
        matrixv(k,m)=MMVN(j,i);
        matrixc1(k,m)=BVN(j,i);
        matrixc2(k,m)=VRN(j,i);
    end
    if (ang>357.5 && (i-1)==0)
        matrixr(k,m)=MMRN(j,i);
        matrixb(k,m)=MMBN(j,i);
        matrixv(k,m)=MMVN(j,i);
        matrixc1(k,m)=BVN(j,i);
        matrixc2(k,m)=VRN(j,i);
    end
elseif angx<0 && angy<=0
    ang=ang+180;
    if (ang>((i-1)-2.5) && ang<((i-1)+2.5))
        matrixr(k,m)=MMRN(j,i);
        matrixb(k,m)=MMBN(j,i);
        matrixv(k,m)=MMVN(j,i);
        matrixc1(k,m)=BVN(j,i);
        matrixc2(k,m)=VRN(j,i);
    end
elseif angx<0 && angy>0
    ang=ang+180;
    if (ang>((i-1)-2.5) && ang<((i-1)+2.5))
        matrixr(k,m)=MMRN(j,i);
        matrixb(k,m)=MMBN(j,i);
        matrixv(k,m)=MMVN(j,i);
        matrixc1(k,m)=BVN(j,i);
        matrixc2(k,m)=VRN(j,i);
    end
end
end
end
end
end
end
end

r=find(matrixr==0);
matrixr(r)=NaN;
b=find(matrixb==0);
matrixb(b)=NaN;
v=find(matrixv==0);
matrixv(v)=NaN;
c1=find(matrixc1==0);
matrixc1(c1)=NaN;
c2=find(matrixc2==0);
matrixc2(c2)=NaN;
figure, contourf(matrixr)
title('R')
figure, contourf(matrixb)
title('B')

```

```
figure, contourf(matrixv)
title('V')
figure, contourf(matrixc1)
title('B-V')
figure, contourf(matrixc2)
title('V-R')
```